ESO-VLT optical spectroscopy of BL Lac objects: II. New redshifts, featureless objects and classification assessments.

B. Sbarufatti[1], A. Treves
Università dell'Insubria, Via Valleggio 11, I-22100 Como, Italy

R. Falomo
INAF, Osservatorio Astronomico di Padova, Vicolo dell'Osservatorio 5, I-35122 Padova, Italy

J. Heidt
Landenssterwarte Heidelberg, Königstuhl, D-69117 Heidelberg, Germany

J. Kotilainen
Tuorla Observatory, University of Turku, Väisäläntie 20, FIN-21500 Piikkiö, Finland

R. Scarpa
European Southern Observatory, 3107 Alonso de Cordova, Santiago, Chile

ABSTRACT

We report on ESO Very Large Telescope optical spectroscopy of 42 BL Lacertae objects of unknown redshift. Nuclear emission lines were observed in 12 objects, while for another six we detected absorption features due to their host galaxy. The new high S/N spectra therefore allow us to measure the redshift of 18 sources. Five of the observed objects were reclassified either as stars or quasars, and one is of uncertain nature. For the remaining 18 the optical spectra appear without intrinsic features in spite of our ability to measure rather faint (EW ∼0.1 Å) spectral lines. For the latter sources a lower limit to the redshift was set exploiting the very fact that the absorption lines of the host galaxy are undetected on the observed spectra.

Subject headings: BL Lacertae objects: general

1. Introduction

BL Lac objects (hereinafter BL Lacs or BLL) are active galactic nuclei (AGN) characterized by luminous, rapidly variable UV–to–NIR non–thermal continuum emission and polarization, strong compact flat spectrum radio emission and superluminal motion. Similar properties are observed also in flat spectrum radio quasars (FSRQ) and the two types of active nuclei are often grouped together in the blazar class. From the spectroscopical point of view BL Lacs are characterized by quasi featureless optical spectra. In fact their spectra are often dominated by the non–thermal continuum that arises from the nucleus. To this emission it is superimposed a thermal contribution due to the stellar component of the host galaxy. Like in other AGN, emission lines could be generated by fluorescence in clouds surrounding the central black hole. Moreover, as it happens for high z quasars in some cases absorption lines due to intervening gas in the halo of foreground

[1]also at Università di Milano-Bicocca

galaxies can be observed in the spectra of BL Lacs and one can derive a lower limit to the redshift of the object. The detectability of spectral features depends on the brightness of the nuclear source: in fact during low brightness states, intrinsic absorption features can be more easily revealed, while during high states one can better discover intervening absorption systems. Because of the strong contribution from the continuum the equivalent width (EW) of all these spectral features is often very small and their detection represents a challenging task.

In the past decade a number of projects were carried out to derive the redshift of BL Lac objects. Most of these works were based on optical spectra collected with 4 m class telescopes, and are therefore limited by relatively low signal-to-noise ratio (S/N), low spectral resolution and limited wavelength range (e.g. Falomo et al. 1993; Stickel & Kühr 1993; Véron-Cetty & Véron 1993; Bade, Fink, & Engels 1994; Falomo, Scarpa, & Bersanelli 1994; Falomo 1996; Marchã et al. 1996; Drinkwater et al. 1997; Laurent-Muehleisen et al. 1998; Landt et al. 2001; Rector & Stocke 2001; Londish et al. 2002; Carangelo et al. 2003; Hook et al. 2003). Recently, however, some observations with 8 m class telescopes were carried out (Heidt et al. 2004; Sowards-Emmerd et al. 2005). Despite these efforts, a significant fraction of known BL Lacs (e. g. 50 % in Véron-Cetty & Véron (2003) catalogue) have still unknown redshift.

In order to improve the knowledge of the redshift of BL Lacs we carried out a project to obtain optical spectra of sources with still unknown or uncertain redshift using the European Southern Observatory (ESO) 8-m Very Large Telescopes (VLT). This allows one to improve significantly the S/N of the spectra and therefore the capability to detect faint spectral features. A first report on this work, giving the redshift of 12 objects, has been presented by Sbarufatti et al. (2005a, Paper I), and here we refer on the results for the full sample of 42 observed sources.

The outline of this paper is the following. In section 2 we give some characterization of the 42 observed objects. The observation and analysis procedures are described in section 3. In sections 4 and 5 we report the results of our spectroscopic study. Finally in section 6 a summary and conclusions of this study are given. Throughout this paper we adopted the following cosmological parameters: H_0= 70 km s^{-1} Mpc^{-1}, Ω_Λ=0.7, Ω_m=0.3.

2. The sample

The sample of BL Lac objects (and candidates) observed with the VLT telescopes was selected from two extended lists of BL Lacs: the Padovani & Giommi (1995a) collection of BL Lacs and the Sedentary Survey (Giommi et al. 1999, 2005, in the following addressed as SS). The Padovani & Giommi (1995a) list contains all objects identified as BL Lacs belonging to the complete samples existing at the time of its compilation, selected in the radio, optical and X-ray bands (e.g.: 1 Jansky survey – 1-Jy, Stickel et al. (1991), Palomar-Green survey – PG, Green et al. (1986), Extended Medium Sensitivity Survey – EMSS, Gioia et al. (1990), Slew survey, Perlman et al. (1996), White-Giommi-Angelini catalogue – WGA White et al. (1994)). It includes also sources from the Hewitt & Burbidge (1993) and Véron-Cetty & Véron (1993) catalogues (in the latter case we checked that the source was still included in the 2001 version), for a total of 233 objects. The criteria used to define a BL Lac object in Padovani & Giommi (1995a) depend on the sample of origin. In most cases, the EW of the lines is required to be $\leq$5 Å, but also UV excess, optical polarization and variability, radio-to-optical spectral index are used as selecting criteria. The SS was obtained cross-correlating the National Radio Astronomy Observatory (NRAO) Very Large Array (VLA) Sky Survey (NVSS) data (Condon et al. 1998) with the ROSAT All Sky Survey–Bright Source Catalogue (RBSC) list of sources (Voges et al. 1999). SS selected a complete sample of 150 High energy peaked BL Lacs (HBL, see Padovani & Giommi 1995b, for definition) down to a 3.5 mJy radio flux limit. BL Lac classification in the SS is based on the position of the sources on the $\alpha_{OX} - \alpha_{RO}$ plane.

The Padovani & Giommi (1995a) and SS datasets lead to a combined list containing 348 objects. The distribution of the V magnitude for these objects is reported in Fig. 1. The bulk of them have V between 15 and 20, and the the fraction of objects with unknown redshift increases with the apparent magnitude and reaches $\sim$ 50% at the faintest magnitudes. Note, however, that also at V $\sim$ 15-17 about 20% of the sources have

not known redshift. The total number of objects with unknown redshifts is 105.

From the combined list we selected sources with δ <+15°, for observability from the VLT site. Moreover to grant a sufficiently high S/N level of the optical spectra we required V<22. Thus we gathered a list of 59 objects. During three observational campaigns, performed in service mode, we completed this optical spectroscopy program, obtaining data for ∼70% of the sample (42 sources). Our sample is similar to the parent sample of 348 objects in terms of mean apparent magnitude and subdivision in Low (LBL) and High energy peaked BL Lacs.

3. Observations and data analysis

Optical spectra were collected in service mode with the FOcal Reducer and low dispersion Spectrograph (FORS1, Appenzeller et al. 1998) on the VLT. The observations were obtained from April 2003 to March 2004 with UT1 (Antu) and from April to October 2004 with UT2 (Kueyen). We used the 300V+I grism combined with a 2" slit, yielding a dispersion of 110 Å/mm (corresponding to 2.64 Å/pixel) and a spectral resolution of 15–20 Å covering the 3800−8000 Å range. The seeing during observations was in the range 0.5−2.5", with an average of ∼1". Relevant informations on the sample objects are given in Table 1.

Data reduction was performed using IRAF[1] (Tody 1986, 1993) following standard procedures for spectral analysis. This includes bias subtraction, flat fielding and cleaning for bad pixels. For each target we obtained three spectra in order to get a good correction of cosmic rays and to check the reality of weak features. The individual frames were then combined into a single average image. Wavelength calibration was performed using the spectra of a Helium/Neon/Argon lamp obtained during the same observing night, reaching an accuracy of ∼ 3 Å(rms). From these images we extracted one-dimensional spectra adopting an optimal extraction algorithm (Horne 1986) to improve the S/N.

[1]IRAF (Image Reduction and Analysis Facility) is distributed by the National Optical Astronomy Observatories, which are operated by the Association of Universities for Research in Astronomy, Inc., under cooperative agreement with the National Science Foundation.

Although this program did not require optimal photometric conditions, most of the observations were obtained with clear sky. This enables us to perform a spectrophotometric calibration of the acquired data using standard stars (Oke 1990) observed in the same nights. From the database of sky conditions at Paranal we estimate that a photometric accuracy of 10% was reached during our observing nights. The spectra were also corrected for Galactic extinction, using the law by Cardelli, Clayton, & Mathis (1989) and assuming values of E_{B-V} from Schlegel, Finkbeiner, & Davis (1998).

4. Results

In Fig. 2 we give the optical spectrum of each source. In order to show more clearly the continuum shape and the faint features we report both the flux calibrated and the normalized spectrum for each object. The main emission and absorption features are identified. Those due to the galactic interstellar gas are indicated as "ISM" and "DIB" (Diffuse Interstellar Bands, see section 4.2.3), while telluric absorptions are marked as ⊕.

4.1. The continuum emission

In a first approximation, the optical continuum of a BL Lac object is due to the superposition of two components: the non-thermal emission of the active nucleus, Doppler-enhanced because of the alignment of the jet with the line of sight, and the emission of the host galaxy. Depending on the relative strength of the nucleus with respect to the galaxy light, the spectral signature of the latter can be either easily detected or diluted beyond the point of recognition. Taking into account the robust evidence that the host galaxies are giant ellipticals (e.g. Urry et al. 2000), to describe the continuum and derive the optical spectral index of the non-thermal component, we fitted a power law ($F_\lambda \propto \lambda^{-\alpha}$, the spectral indices are given in Table 1) plus the spectrum of a typical elliptical galaxy as described by the Kinney et al. (1996) template. While in most cases the contribution of the host galaxy was negligible, in 6 sources it was not, and the luminosity of the host can thus be derived. For these six sources (three of them were presented in Paper I) we give the best fit decomposition in Fig.3 and report the parameters in Table 2. The derived absolute magnitudes of the host galaxies

are consistent with the distribution of M_R of BL Lac hosts given by Sbarufatti et al. (2005b).

4.2. Spectral features and redshifts

The detection and the measurement of very weak spectral features is difficult to assess because it depends on the choice of the parameters used to define the spectral line and the continuum. In order to apply an objective method for any given spectrum we evaluate the minimum measurable equivalent width (EW_{min}) defined as twice the rms of the distribution of all EW values measured dividing the normalized spectrum into 30 Å wide bins (details for this automatic routine are given in Paper I). We checked that the S/N ratio dependence inside the considered spectral range varies at most by 20 %, remaining <10% over a large wavelength range. This reflects into a similar variation of EW_{min}. The procedure for calculating EW_{min} was applied to all featureless or quasi-featureless spectra to find faint spectral lines. All features above the EW_{min} threshold, ranging from $\sim$ 1 Å to 0.1 Å in our data, were considered as line candidates and were carefully visually inspected and measured. The results are summarized in Tab. 1. Based on the detected lines and the shape of the continuum we confirm the BL Lac classification for 36 objects, while 6 sources were reclassified. Depending on the observed spectral properties the objects can be assembled in three groups.

4.2.1. Confirmed BL Lacs with measured z.

Twelve objects belonging to this group were reported in paper I. Six more are presented here (Table 1). Three have redshift derived from emission lines (0723–008, z=0.128; 2131–021, z=1.284; 2223–114, z=0.997) and three from absorption lines (1212+078, z=0.137; 1248–296, z=0.382; 2214–313, z=0.460). Details on each source are given in section 5.

4.2.2. Misclassified and uncertain nature objects.

Despite their classification as BL Lac objects in one or more input catalogues, six sources have spectra incompatible with this identification. Five of them were reclassified either as quasars (0420+022, 1320+084) or stars (1210+121, 1222+102, 1319+019), while object 0841+129 remains of uncertain nature.

4.2.3. Lineless BL Lacs.

In spite of the high S/N 18 objects exhibit spectra lacking any intrinsic feature. In several spectra we clearly see absorption features from the interstellar medium (ISM) of our Galaxy. In particular, we are able to detect CaII $\lambda\lambda$3934,3968, NaI λ5892 atomic lines, and a number of DIBs $\lambda\lambda$ 4428,4726,4882,5772, generated by complex molecules in the ISM (e.g. Galazutdinov et al. 2000, and references therein). In Fig. 4 we report the average spectrum of the interstellar absorptions. In three cases absorption lines from intervening gas are detected, leading to lower limits on the redshift of the objects (0841+129, z>2.48; 2133–449, z>0.52; 2233–148, z>0.49).

For these 18 sources we have estimated a redshift lower limit based on the EW_{min} of their spectra and the apparent magnitudes of the nuclei. We report **these** in Table 1. The procedure to obtain these limits is described in section 4.2.4.

4.2.4. Redshift lower limits procedure.

In this section we describe the procedure to obtain redshift lower limits for BL Lacs with lineless spectra (see Table 1) from the EW_{min} of the spectrum and the observed magnitude of the object. Under the assumption that the host galaxy luminosity is confined in a narrow range (Sbarufatti et al. 2005b) it is in fact possible to constrain the position of the source on the nucleus-to-host flux ratio (ρ) *vs* redshift plane.

We assume that the observed spectrum of a BL Lac object is given by the contribution of two components: 1- a non-thermal emission from the nucleus that can be described by a power law ($F(\lambda) = C\lambda^{-\alpha}$, where C is the normalization constant); 2 - a thermal component due to the host galaxy. Depending on the relative contribution of the two components the optical spectrum will be dominated by the non-thermal (featureless) emission or by the spectral signature of the host galaxy. The observed equivalent width (EW_{obs}) of a given spectral absorption line is diluted depending on the ratio of the two components. Detection of this spectral feature requires a spectrum with a sufficiently high S/N. This is illustrated in Fig 5, where

a simulated spectrum (ρ=5, z=0.5) is reproduced with two different S/N ratios. The S/N=300 spectrum grants a secure detection of the CaII features, while with S/N=30 the lines are undetected.

In order to estimate the redshift of an object from the EW_{min} we need to know the relation between EW_{obs} and the nucleus-to-host flux ratio ρ. For a spectral absorption line of intrinsic equivalent width EW_0 the observed equivalent width is given by the relation (see also Sbarufatti 2005):

$$EW_{obs} = \frac{(1+z) \times EW_0}{1 + \rho \times A(z)} \quad (1)$$

The nucleus-to host ratio ρ can be represented by

$$\rho(\lambda) = \frac{F(\lambda)}{G(\lambda)} \quad (2)$$

where $G(\lambda)$ is the giant elliptical spectral template by Kinney et al. (1996, see also section 4.1), and A(z) is a correction term that takes into account the loss of light inside the observed aperture. In this work the aperture is a 2"×6" slit that captures $\gtrsim$ 90% of the nuclear light, but not the whole surrounding galaxy that is more extended than the aperture (in particular for low z targets). In order to estimate this effect we evaluated the amount of light lost from the galaxy through the aperture in use from simulated images of BL Lacs (point source plus the host galaxy). The main parameters involved are the shape and the size of the host galaxy. According to the most extensive imaging studies of BLL (Falomo 1996; Wurtz et al. 1996; Falomo & Kotilainen 1999; Heidt et al. 1999; Nilsson et al. 2003; Urry et al. 2000) we assumed that the host galaxy is a giant elliptical of effective radius R_e= 10 kpc. The fraction of starlight lost then depends on the redshift of the object and is particularly significant at z< 0.2, producing the bending of the curves in Fig. 6.

Since we want to refer the observed equivalent width to the nucleus-to-host ratio $\rho_0 = \rho(\lambda_0)$ at a fixed wavelength λ_0, equation (1) can be rewritten as:

$$EW_{obs} = \frac{(1+z) \times EW_0}{1 + \rho_0 \times \Delta \times A(z)} \quad (3)$$

where $\Delta(\lambda)$ is the nucleus-to-host ratio normalized to that at λ_0 ($\Delta(\lambda) = \rho(\lambda)/\rho(\lambda_0)$; see Fig. 7).

On the other hand the quantity ρ_0 depends also on the observed magnitudes of the object, since

$$\log(\rho_0) = -0.4[M_n(z) - M_h(z)] \quad (4)$$

where M_n is the nucleus absolute magnitude and M_h is the host absolute magnitude, and

$$M_n(z) = m_n + 5 - 5\log d_l(z) - k_n(z) \quad (5)$$

where m_n is the nucleus apparent magnitude, $d_L(z)$ is the luminosity distance and $k_n(z)$ is the nucleus k-correction, computed following Wisotzki (2000). The absolute magnitude of the host is

$$M_h(z) = M_h^* - E(z) \quad (6)$$

where M_h^*=–22.9 is the average R band magnitude of BL Lac hosts at z=0 and E(z) is the evolution correction, as given by Bressan et al. (1998).

An example of the procedure described above is given in Fig. 8, where the relationships between $\log(\rho_0)$ and the redshift for a given value of EW_{min} and m_n are shown. The intersection of the two curves yields a lower limit to the redshift of the target. When it goes beyond the observed spectral range, we set the redshift limit to the value corresponding to the considered feature reaching the upper limit of the observed wavelength range (z∼1 in the case of CaII λ3934 line). The uncertainty of this procedure depends mainly on the spread of the distribution of the host galaxy luminosity. This issue is discussed in Urry et al. (2000) and in Sbarufatti et al. (2005b), where it is shown that the 64 BL Lacs hosts of known redshift resolved with HST are well represented by an elliptical of M_R=-22.9, with 68% of them in the interval -23.4 – -22.4.

This procedure can be used for any absorption line belonging to the host galaxy and for which an estimate of the un-diluted EW is available. In this work we considered the CaII absorption line at λ=3934 Å(EW_0=16 Å), we assumed a power law spectral index α=0.7 (Falomo et al. 1993), and we referred to the effective wavelength of the R band (λ_0=6750 Å) to compute ρ_0 (which implies Δ=4.3).

In order to test this procedure we considered eight BL Lacs for which the CaII line of the host galaxy has been measured. Five of these objects derive from the observations discussed here and

in paper I, three others are from observations obtained at the ESO 3.6 (Carangelo et al. 2003; Sbarufatti 2005). These spectra are reported in Fig. 9 and the relevant parameters are given in Table 4. The comparison between the redshifts estimated by our procedure with the spectroscopic ones indicates a reasonable good agreement (see Fig. 10).

5. Notes to individual objects.

0047+023 This compact and flat spectrum radio source was classified as a BL Lac by Hewitt & Burbidge (1993) on the basis of UV color and featureless spectra. Further featureless optical spectra obtained by Allington-Smith et al. (1991); Véron-Cetty & Véron (1993) confirmed the BL Lac. Even in our S/N$\sim$ 80 spectrum no spectral features were found. Based on the minimum detectable EW the source is most likely at z > 0.82.

0048–097 Previous optical observations of this well known BL Lac object belonging to the 1-Jy sample, reported a featureless spectrum (Stickel et al. 1991; Falomo, Scarpa, & Bersanelli 1994). Rector & Stocke (2001), however, suggested the presence of an emission line at 6092 Å (possibly identified with [OII] λ3727 at z=0.634 or [OII] λ5007 at z=0.216). Falomo (1996) proposed z>0.5, based on the non detection of the host galaxy in the optical images of the source. Our S/N=250 optical spectrum does not confirm the presence of the emission line at 6092 Å, and apart of some telluric lines and a number of Galactic absorptions it is found featureless. From our EW$_{min}$ estimate, we infer that this source is at z>0.3.

0420+022 Fricke et al. (1983) classified this source as a BL Lac candidate on the basis of a featureless (although noisy) optical spectrum. Ellison et al. (2001) through an unpublished optical spectrum propose a redshift z=2.277 and classify the source as a radio loud QSO. In our optical spectrum we are able to clearly detect emission lines Ly$_\alpha$ λ1419 OVI] λ1034, CIV λ1549 and CIII] λ1909, at z = 2.278. A recent spectrum obtained by Hook et al. (2003) also confirm our findings and the classification of the object as a QSO.

0422+004 This object is a well known radio selected BL Lac, included in the Hewitt & Burbidge (1993) catalogue. Falomo (1996) detected the host galaxy with ground-based imaging, proposing z$\sim$0.2–0.3. The optical spectrum taken by Falomo, Scarpa, & Bersanelli (1994) is featureless. Our spectrum (S/N=230) does not show evidence for intrinsic spectral features from the host, suggesting a very high N/H ratio. Interstellar absorptions from NaI λ5892 and DIBs at 5772 and 4726 Å are well detected. Based on EW$_{min}$, we estimate z>0.31.

0627–199 Hook et al. (2003) obtained a lineless spectrum for this radio selected BL Lac object. Our VLT spectrum, of moderate S/N (50), shows no spectral features. From EW$_{min}$we set z>0.63.

0723–008 Wills & Wills (1976) classified this source as a Narrow Emission Line Radio Galaxy based on an optical spectrum, giving z=0.127. Rusk & Seaquist (1985) report an optical polarization of 1.5 %, classifying the source as a Low Polarization QSO. Véron-Cetty & Véron (2001) report this source as a BL Lac object. Henriksen et al. (1984) gives broad band indices α_{RO}=0.7 and α_{OX}=1.0, which are compatible with a BL Lac or a FSRQ classification. Our optical spectrum is clearly dominated by a non thermal emission with spectral index α=0.7. Superposed to this, strong narrow emission lines and absorption lines from the underlying host galaxy at z=0.127 are detected, confirming the redshift. From the values of the spectral indices and the measured EW for the spectral lines, we suggest that this object is of intermediate nature between a BL Lac and a quasar.

0841+129 This source, first identified by C. Hazard (see Jaunsen et al. 1995, and references therein), is a Damped Lyman α Absorption (DLA) QSO at z>2.48 as derived from the two very strong DLAs at $\sim$4100 and $\sim$4225 Å (see for example Pettini et al. 1997; Prochaska et al. 2001; Warren et al. 2001, and references therein). The classification as a BL Lac object was motivated by the absence of prominent emission lines (Hewitt & Burbidge 1993).

Our spectrum, in addition to several absorption lines, exhibit three possible broad emission structures at$\sim$4310, $\sim$4850 and $\sim$5370 Å. These could

be interpreted as NV λ1240, SiIV λ1397 and CIV λ1549 at z$\sim$2.47. This is consistent with z$\sim$2.5, deduced from the observed position of the onset of the absorption of the Ly$_\alpha$ forest Warren et al. (2001). An alternative explanation is, however, that these structures are pseudo-emissions resulting from the depression of the continuum caused by the envelope of many unresolved narrow absorption features. Higher resolution spectra of the object in the spectral range 4200 to 5800 Å are needed to distinguish between the two possibilities.

1210+121 Hazard & Murdoch (1977) proposed that this object was the optical counterpart of a radio source in the Molongo Catalogue (MC2 Sutton et al. 1974); the separation was however 16". Zotov & Tapia (1979) reported large optical variability and polarization, apparently reinforcing the identification. Baldwin et al. (1973) found a featureless optical spectrum. Our VLT spectrum clearly shows that the source is a type B star in our Galaxy.

1212+078 Our VLT spectrum clearly shows the presence of a strong thermal component due to the host. We detected CaII $\lambda\lambda$3934, 3968, G band λ4305, MgI λ5175 and H$_\alpha$ λ6563 in emission at z=0.137, confirming the redshift estimated by Perlman et al. (1996). The contribution of the non-thermal component is visible in the bluest part of the spectrum. The best fit decomposition of the spectrum gives α=1.17 for the non-thermal component and M$_R$=-22.0 for the host. Though this is somewhat fainter than expected for a BL Lac host galaxy, we can not exclude that given the low redshift and the consequent large apparent size of the host, part of the light did not enter in the slit.

1222+102 This is a blue stellar object in the direction of the Virgo-Coma cluster. Its apparent position in the sky is very close to the center of the galaxy NGC 4380, still well inside the galaxy boundaries. The projected separation to the nucleus at the redshift of the galaxy is $\sim$10 kpc. The object is considered a candidate BL Lac in the Burbidge & Hewitt (1987) list, selected because of its UV excess. Arp (1977) reports the observation of a featureless spectrum. Burbidge (1996) estimates this object a possible candidate of expulsion from a galactic nucleus. The sharp absorption lines detected in our spectrum clearly indicate a stellar origin. The measured colors lead to a temperature of $\sim$10000 K. If the object were a main sequence or a supergiant star, the corresponding distance will put it outside the Galaxy, but not at the distance of NGC 4380. We are therefore led to consider a white dwarf, which would be at 100–200 pc. The absence of H lines indicates a DQ or DXP white dwarf (Schmidt et al. 2001, 2003). Some of the lines are referable to HeI and CI transitions. The object clearly deserves further study; in particular polarization measurements would be interesting.

1248–296 Perlman et al. (1996) obtained a low S/N spectrum of this source, and proposed a BL Lac at z=0.487 based on the possible detection of the host galaxy features. In our VLT spectrum CaII, G band, H$_\beta$ are clearly detected at z=0.382, confirming the findings of Woo et al. (2005), while in the blue part the contribution of a non-thermal component is clearly visible. The best fit decomposition gives α=0.92 for the non-thermal component visible below 5000 Å, and M$_R$=-22.7 for the host, in good agreement with result from the direct detection of the host in HST imaging (Urry et al. 2000; Sbarufatti et al. 2005b).

1319+019 This object was initially selected as a BL Lac candidate on the basis of the University of Michigan objective prism survey (MacAlphine & Williams 1981) designed to find AGN and it is included as BL Lac in the Véron-Cetty & Véron (2001) catalogue. No radio counterpart for this source has been found in literature. Later Thompson & Djorgovski (1990) proposed its classification as a BL Lac, based on a low S/N optical spectrum that was found featureless. In our much better quality spectrum we clearly see many absorption features that characterize the object as a galactic star of spectral type $\sim$A. Our findings are also in agreement with the spectral classification of the 2dF QSO Redshift survey (2QZ, see Croom et al. 2004).

1320+084 This source is part of the BL Lac sample extracted from the EINSTEIN Slew Survey and a radio counterpart was reported by Perlman et al. (1996). Our VLT data show the source has a QSO like spectrum at z=1.5, in contrast with a featureless spectrum observed by Perlman et al. (1996). Several intervening absorption lines, in particular MgII at z=1.347 were also detected.

1349–439 The spectrum of this X-ray selected BL Lac (della Ceca et al. 1990), shows a number of absorption lines from the interstellar medium: CaII $\lambda\lambda$3934,3968, the 5772 Å DIB, NaI λ5892. No intrinsic features were detected, and the deduced redshift lower limit is z>0.39. As already pointed out by Véron (1996), the value z=0.05 sometime reported for this object is consequence of a confusion with the nearby Seyfert 1 galaxy Q 1349-439.

1442–032 This X-ray source, the radio counterpart of which was found in the NVSS survey, was first classified as a BL Lac in the RBSC-NVSS sample by Bauer et al. (2000), and then confirmed by the SS. There are no published optical spectra for this source. Our optical spectrum is featureless, with the exception of the NaI λ5892 absorption feature from our galaxy ISM. The EW$_{min}$ value for this objects leads to z>0.51.

1500-154 This X-ray selected BL Lac is part of the RSBC-NVSS sample (Bauer et al. 2000) and enters in SS. No previous optical spectroscopy has been found in the literature. Our spectrum is completely featureless, leading to z> 0.38 from the obtained EW$_{min}$.

1553+113 This source is an optically selected BL Lac from the Palomar-Green survey. The redshift estimate z=0.360 given in the Hewitt & Burbidge (1993) catalogue was disproved by later spectroscopy (Falomo & Treves 1990; Falomo, Scarpa, & Bersanelli 1994). While no intrinsic features were detected in our S/N=250 VLT spectrum, a number of absorption lines due to our galaxy ISM were revealed: CaII $\lambda\lambda$3934,3968, NaI λ5892 and DIBs at 4428,4726,4882,5772 Å. The EW$_{min}$ estimate for this object gives a limit z>0.09.

1722+119 Griffiths et al. (1989) reported a tentative redshift z=0.018 for this X-ray selected, highly polarized BL Lac. This estimate was not confirmed by more recent observations (Véron-Cetty & Véron 1993; Falomo et al. 1993; Falomo, Scarpa, & Bersanelli 1994). Our VLT spectrum (S/N=350) shows only absorption features due to our galaxy ISM: CaII $\lambda\lambda$3934,3968, NaI λ5892 and DIBs at 4428 Å, 4726 Å, 4882 Å, 5772 Å, with no evidence of intrinsic features. From the minimum EW$_{min}$ we derive z>0.17.

2012–017 Consistently with previous observations of this radio selected BL Lac (White et al. 1988; Véron et al. 1990; Falomo, Scarpa, & Bersanelli 1994), also our S/N=130 VLT spectrum is featureless. The optical spectral index is α=0.49, in marginal agreement with α=0.33±0.12 reported by Falomo, Scarpa, & Bersanelli (1994). From EW$_{min}$ we derive z>0.94.

2128–254 The spectrum of this X-ray selected BL Lac candidate is reported as featureless by SS. We confirm this result and set a lower limit of z>0.86 for the redshift.

2131–021 Rector & Stocke (2001) and Drinkwater et al. (1997) proposed a redshift of 1.285 for this source, based on the detection of CIII] λ1909, MgII λ2798 and [OII] λ3727, opposed to the z=0.557 suggested by Wills & Wills (1976). While [OII] falls outside our spectral range, we confirm the presence of CIII] and MgII emission lines at z=1.283, also detecting the fainter CII] λ2326 feature at the same redshift.

2133–449 This source was discovered because of its optical variability by Hawkins et al. (1991). Optical spectroscopy by Hawkins et al. (1991) and Heidt et al. (2004) led to completely featureless spectra. Our VLT observations clearly show the presence of an intervening absorption feature at 4250 Å, a tentative identification of which is intervening MgII at z=0.52 (see Churchill et al. 2005). The lower limit on z derived from EW$_{min}$ is z>0.98 .

2136–428 The spectrum obtained by Hawkins et al. (1991), who discovered this source study-

ing its optical variability, is completely featureless. Our VLT observations shows several absorption features due to the ISM of our galaxy: DIB at 4428 Å, 4726 Å, 4882 Å and 5772 Å, CaII $\lambda\lambda$3934, 3968 and NaIλ 5892 atomic lines. The feature at 5942 Å could be CaII λ3968 at z=0.497. Since at this redshift the CaII λ3934 should fall at 5890 Å, where it will be strongly contaminated by the interstellar NaI absorption, the redshift estimate is only tentative. The lower limit deduced by the minimum measurable EW is z>0.24.

2214–313 Our VLT spectrum of this object clearly shows the typical spectral signature of the host galaxy (CaII $\lambda\lambda$3934,3968 and G band λ4305) at z=0.46. The best fit decomposition gives α=0.9 for the non-thermal component and M_R=–22.3 for the host. Previous optical spectroscopy performed by Bade, Fink, & Engels (1994) with the ESO 3.6m telescope failed to detect any spectral feature.

2223–114 Optical observations of this radio source obtained by Véron-Cetty & Véron (1993) did not show any intrinsic spectral feature. In our spectrum, that extends further in the red, we detect a single narrow emission line at λ7367 (EW = 5 Å). This is a real feature since it clearly appears on each of the 3 individual spectra (see section 3). A possible identification of this line is [OII]λ 3727 at z=0.977, while MgII λ2798 gives z=1.633. We discarded this second classification because the line FWHM (1200 km s^{-1}), is typical for a narrow line such [OII], while for MgII a larger value would be expected. Moreover, with a MgII identification both CIV λ1549 and CIII] λ1909 broad lines would be expected inside the observed spectral range, but no other features are detected.

2233–148 The redshift z=0.325 reported by Johnston et al. (1995) is due to confusion with the source HB89 2233+134 in Schmidt & Green (1983). Drinkwater et al. (1997) report an intervening system at z=0.609, but without giving an identification of the corresponding absorption feature. We detect several absorption features on the spectrum. In particular we propose to identify the features at 4165 and 4183 Å as MgII at z=0.492, while, using the EW_{min} estimate from the spectrum, z>0.65 is found.

2254–204 Previous optical spectroscopy (Véron-Cetty & Véron 1993; Hook et al. 2003) of this BL Lac object from the 1Jy sample showed completely featureless spectra. With VLT we are able to detect faint interstellar absorptions of CaII $\lambda\lambda$3934, 3968 and NaIλ 5892, but no intrinsic or intervening spectral lines are found. The inferred redshift limit is z>0.47.

2307–375 This source was first classified as a BL Lac in the RSBC-NVSS sample (Bauer et al. 2000). The classification was then confirmed by the SS. No previous optical spectroscopy has been published. Our VLT spectrum is featureless, allowing us to set only a lower limit to the redshift of z>1.

2342–153 This source is part of the EMSS sample of BL Lac objects. Our VLT data, as well as previous optical spectroscopy with the 6.5 m telescope of Multi Mirror Telescope Observatory (Rector et al. 2000) showed a featureless spectrum. From EW_{min} we derive z>1.

2354–021 This object was discussed in paper I. Here we report only the spectrum, in Fig. 2.

2354–175 This X-ray source from ROSAT All Sky Survey, is classified as BL Lac candidate in the RBSC-NVSS sample (Bauer et al. 2000) and in the SS. No previous spectroscopy was published in literature. Our S/N=150 VLT spectrum is featureless, allowing only to set a lower limit of z>0.85 to the redshift.

6. Summary and conclusions

Out of 42 objects observed we confirm the BL Lac classification for 36 sources and for 18 of them we are able to measure/confirm the redshift. This information allows us to derive the luminosity of the objects. The distribution in the V band luminosity-distance plane is indeed fully consistent with what observed for BL Lacs of known redshift in the combination of the Padovani & Giommi (1995a) and the SS sample (see Fig. 11).

We note that the sources in this combined list are affected by the typical selection effect of incomplete, flux limited samples: the envelope of the objects follows in fact the expected behavior for sources with constant V magnitude, centered around V=18, with a spread of ~ 3 mag. The objects discussed here (filled circles and lower limits) follow the same distribution, with absolute magnitudes ranging between -21.5 and -27.5, slightly increasing with the redshift.

In 18 cases the optical spectra remain lineless in spite of the high S/N of the obtained optical spectra. This indicates that if they are hosted by galaxies of standard luminosity they have likely very luminous or extremely beamed nuclei (see also Sbarufatti et al. 2005b). In the latter case one may expect to see the most extreme cases of relativistic beaming, making these sources ideal targets for milli-arcsec resolution radio observations. Alternatively, if the host galaxies were under-luminous, these objects could be rare examples of dwarf galaxies hosting an AGN (see Sbarufatti et al. 2005b).

The high S/N of most of the optical spectra obtained at VLT represents a frontier for the determination of the redshift of BL Lacs with current instrumentation and further improvement of the issue will not be easy to get. In particular the four brightest objects (R<16: 0048–099, 1553+113, 1722+119, 2136-428) we observed at the VLT have values of EW_{min} smaller than 0.25 Å. These objects belong to an interesting subpopulation of BL Lac objects with extreme nuclear (and/or host) properties for which it is actually not possible to derive the intrinsic physical parameters. One possibility is to image the source when it is particularly faint in order to improve the detection of the host galaxy and to derive an imaging redshift (Sbarufatti et al. 2005b). Deep spectroscopic observations in the near-IR may also prove to be effective in the determination of the redshift considering this region of the spectrum is poorly known.

We would like to thank the referee, Dr. John Stocke, for his accurate and helpful comments, which allowed us to improve the quality of this work.

REFERENCES

Abraham, R. G., Crawford, C. S., & McHardy, I. M. 1991, MNRAS, 252, 482

Allington-Smith, J. R., Peacock, J. A., & Dunlop, J. S. 1991, MNRAS, 253, 287

Appenzeller et al., 1998, Messenger 94, 1

Arp, H. 1977, Coll. Intl. No. 263, Paris-Centre Nat. Recherche Sci, p. 377

Bade, N., Fink, H. H., & Engels, D. 1994, A&A, 286, 381

Bauer, F. E., Condon, J. J., Thuan, T. X., & Broderick, J. J. 2000, ApJS, 129, 547

Baldwin, J. A., Burbidge, E. M., Hazard, C., Murdoch, H. S., Robinson, L. B., & Wampler, E. J. 1973, ApJ, 185, 739

Bressan, A., Granato, G. L., & Silva, L. 1998, A&A, 332, 135

Burbidge, G., & Hewitt, A. 1987, AJ, 93, 1

Burbidge, G. 1996, A&A, 309, 9

Carangelo, N., Falomo, R., Kotilainen, J., Treves, A., & Ulrich, M.-H. 2003, A&A, 412, 651

Cardelli, J. A., Clayton, G. C., & Mathis, J. S. 1989, ApJ, 345, 245

Churchill, C. W., Kacprzac, G. G. & Steidel, C. C., 2005, proceedings for IAU colloquium 199: Probing Galaxies through Quasar Absorption Lines, Cambridge University Press, 2005

Condon, J. J., Cotton, W. D., Greisen, E. W., Yin, Q. F., Perley, R. A., Taylor, G. B., & Broderick, J. J. 1998, AJ, 115, 1693

Croom, S. M., Smith, R. J., Boyle, B. J., Shanks, T., Miller, L., Outram, P. J., & Loaring, N. S. 2004, MNRAS, 349, 1397

della Ceca, R., Palumbo, G. G. C., Persic, M., Boldt, E. A., Marshall, E. E., & de Zotti, G. 1990, ApJS, 72, 471

Drinkwater, M. J., et al. 1997, MNRAS, 284, 85

Ellison, S. L., Yan, L., Hook, I. M., Pettini, M., Wall, J. V., & Shaver, P. 2001, A&A, 379, 393

Falomo, R., & Treves, A. 1990, PASP, 102, 1120

Falomo, R., Bersanelli, M., Bouchet, P., & Tanzi, E. G. 1993, AJ, 106, 11

Falomo, R., Scarpa, R., & Bersanelli, M. 1994, ApJS, 93, 125

Falomo, R. 1996, MNRAS, 283, 241

Falomo, R. & Kotilainen, J.K. 1999, A&A, 352, 85

Falomo, R., Kotilainen, J. K., Carangelo, N., & Treves, A. 2003, ApJ, 595, 624

Fricke, K. J., Kollatschny, W., & Witzel, A. 1983, A&A, 117, 60

Galazutdinov, G. A., Musaev, F. A., Krełowski, J., & Walker, G. A. H. 2000, PASP, 112, 648

Gioia, I. M., Maccacaro, T., Schild, R. E., Wolter, A., Stocke, J. T., Morris, S. L., & Henry, J. P. 1990, ApJS, 72, 567

Giommi, P., Menna, M. T., & Padovani, P. 1999, MNRAS, 310, 465

Giommi, P., Piranomonte, S., Perri, M., & Padovani, P. 2005, A&A, 434, 385

Green, R. F., Schmidt, M., & Liebert, J. 1986, ApJS, 61, 305

Griffiths, R. E., Wilson, A. S., Ward, M. J., Tapia, S., & Ulvestad, J. S. 1989, MNRAS, 240, 33

Hawkins, M. R. S., Veron, P., Hunstead, R. W., & Burgess, A. M. 1991, A&A, 248, 421

Hazard, C., & Murdoch, H. S. 1977, Australian Journal of Physics Astrophysical Supplement, 42, 1

Heidt, J., Nilsson, K., Sillanpää, A., Takalo, L. O., & Pursimo, T. 1999, A&A, 341, 683

Heidt, J., Tröller, M., Nilsson, K., Jäger, K., Takalo, L., Rekola, R., & Sillanpää, A. 2004, A&A, 418, 813

Henriksen, M. J., Marshall, F. E., & Mushotzky, R. F. 1984, ApJ, 284, 491

Hewitt, A., & Burbidge, G. 1989, ApJS, 69, 1

Hewitt, A., & Burbidge, G. 1993, ApJS, 87, 451

Hook, I. M., Shaver, P. A., Jackson, C. A., Wall, J. V., & Kellermann, K. I. 2003, A&A, 399, 469

Horne, K., 1986, PASP, 98, 609

Jaunsen, A. O., Jablonski, M., Pettersen, B. R., & Stabell, R. 1995, A&A, 300, 323

Johnston, K. J., et al. 1995, AJ, 110, 880

Kinney, A. L., Calzetti, D., Bohlin, R. C., McQuade, K., Storchi-Bergmann, T., & Schmitt, H. R. 1996, ApJ, 467, 38

Landt, H., Padovani, P., Perlman, E. S., Giommi, P., Bignall, H., & Tzioumis, A. 2001, MNRAS, 323, 757

Laurent-Muehleisen, S. A., Kollgaard, R. I., Ciardullo, R., Feigelson, E. D., Brinkmann, W., & Siebert, J. 1998, ApJS, 118, 127

Londish, D., et al. 2002, MNRAS, 334, 941

Marchã, M. J. M., Browne, I. W. A., Impey, C. D., & Smith, P. S. 1996, MNRAS, 281, 425

MacAlphine, G. M., & Williams, G. A. 1981, ApJS, 45, 113

Nilsson, K., Pursimo, T., Heidt, J., Takalo, L. O., Sillanpää, A., & Brinkmann, W. 2003 A&A, 400, 95

Oke, J. B. 1990, AJ, 99, 1621

Padovani, P., & Giommi, P. 1995a, MNRAS, 277, 1477

Padovani, P., & Giommi, P. 1995b, ApJ, 444, 567

Perlman, E. S., et al. 1996, ApJS, 104, 251

Pettini, M., Smith, L. J., King, D. L., & Hunstead, R. W. 1997, ApJ, 486, 665

Prochaska, J. X., et al. 2001, ApJS, 137, 21

Rector, T. A., Stocke, J. T., Perlman, E. S., Morris, S. L., & Gioia, I. M. 2000, AJ, 120, 1626

Rector, T. A., & Stocke, J. T. 2001, AJ, 122, 565

Rusk, R., & Seaquist, E. R. 1985, AJ, 90, 30

Sbarufatti, B. 2005, PhD thesis, University of Milano-Bicocca

Sbarufatti, B., Treves, A., Falomo, R., Heidt, J., Kotilainen, J., Scarpa, R. 2005a , AJ, 129, 599 (Paper I)

Sbarufatti, B., Treves, A., Falomo, R. 2005b, ApJ, 635, 173

Schlegel, D. J., Finkbeiner, D. P., & Davis, M. 1998, ApJ, 500, 525

Schmidt, M., & Green, R. F. 1983, ApJ, 269, 352

Schmidt, G. D., et al. 2003, ApJ, 595, 1101

Schmidt, G. D., Vennes, S., Wickramasinghe, D. T., & Ferrario, L. 2001, MNRAS, 328, 203

Sowards-Emmerd, D., Romani, R. W., Michelson, P. F., Healey, S. E., Nolan, P. L., ApJ, 626, 95

Stickel, M., Fried, J. W., Kühr, H., Padovani, P., & Urry, C. M. 1991, ApJ, 374, 431

Stickel, M., & Kühr, H. 1993, A&AS, 100, 395

Sutton, J. M., Davies, I. M., Little, A. G., & Murdoch, H. S. 1974, Australian Journal of Physics Astrophysical Supplement, 33, 1

Thompson, D. J., & Djorgovski, S. 1990, PASP, 102, 959

Tody, D. 1993, ASP Conf. Ser. 52: Astronomical Data Analysis Software and Systems II, 2, 173

Tody, D. 1986, Proc. SPIE, 627, 733

Urry, C. M., Scarpa, R., O'Dowd, M., Falomo, R., Pesce, J. E., & Treves, A. 2000, ApJ, 532, 816

Véron, P. 1996, A&A, 310, 381

Véron, P., Véron-Cetty, M.-P., Djorgovski, S., Magain, P., Meylan, G., & Surdej, J. 1990, A&AS, 86, 543

Véron-Cetty, M.-P., & Véron, P. 1993, ESO Scientific Report, Garching: European Southern Observatory (ESO), 1993, 6th ed.,

Véron-Cetty, M.-P., & Véron, P. 1993, A&AS, 100, 521

Véron-Cetty, M.-P., & Véron, P. 2001, A&A, 374, 92

Véron-Cetty, M.-P., & Véron, P. 2003, A&A, 412, 399

Voges, W., et al. 1999, A&A, 349, 389

Warren, S. J., Møller, P., Fall, S. M., & Jakobsen, P. 2001, MNRAS, 326, 759

Weiler, K. W., & Johnston, K. J. 1980, MNRAS, 190, 269

White, G. L., Jauncey, D. L., Wright, A. E., Batty, M. J., Savage, A., Peterson, B. A., & Gulkis, S. 1988, ApJ, 327, 561

White, N. E., Giommi, P., & Angelini, L. 1994, IAU Circ., 6100, 1

Wills, D., & Wills, B. J. 1976, ApJS, 31, 143

Wisotzki, L. 2000, A&A, 353, 861

Woo, J.-H., Urry, M. C., van der Marel, R. P., Lira, P., Maza, J., 2005, ApJ, 631, 762

Wurtz, R., Stocke, J. T., & Yee, H. K. C. 1996, ApJS, 103, 109

Zotov, N. V., & Tapia, S. 1979, ApJ, 229, L5

This 2-column preprint was prepared with the AAS LaTeX macros v5.2.

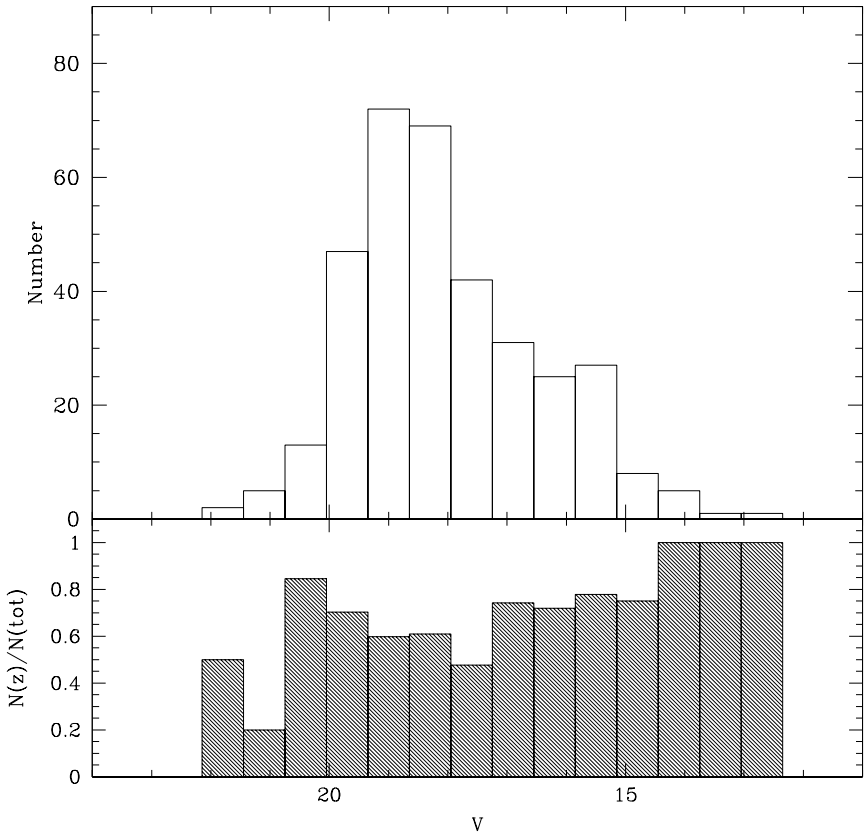

Fig. 1.— Upper panel: V magnitude distribution of BL Lac objects from Padovani & Giommi (1995a) and SS. Lower panel: fraction of objects of known redshift as a function of the magnitude.

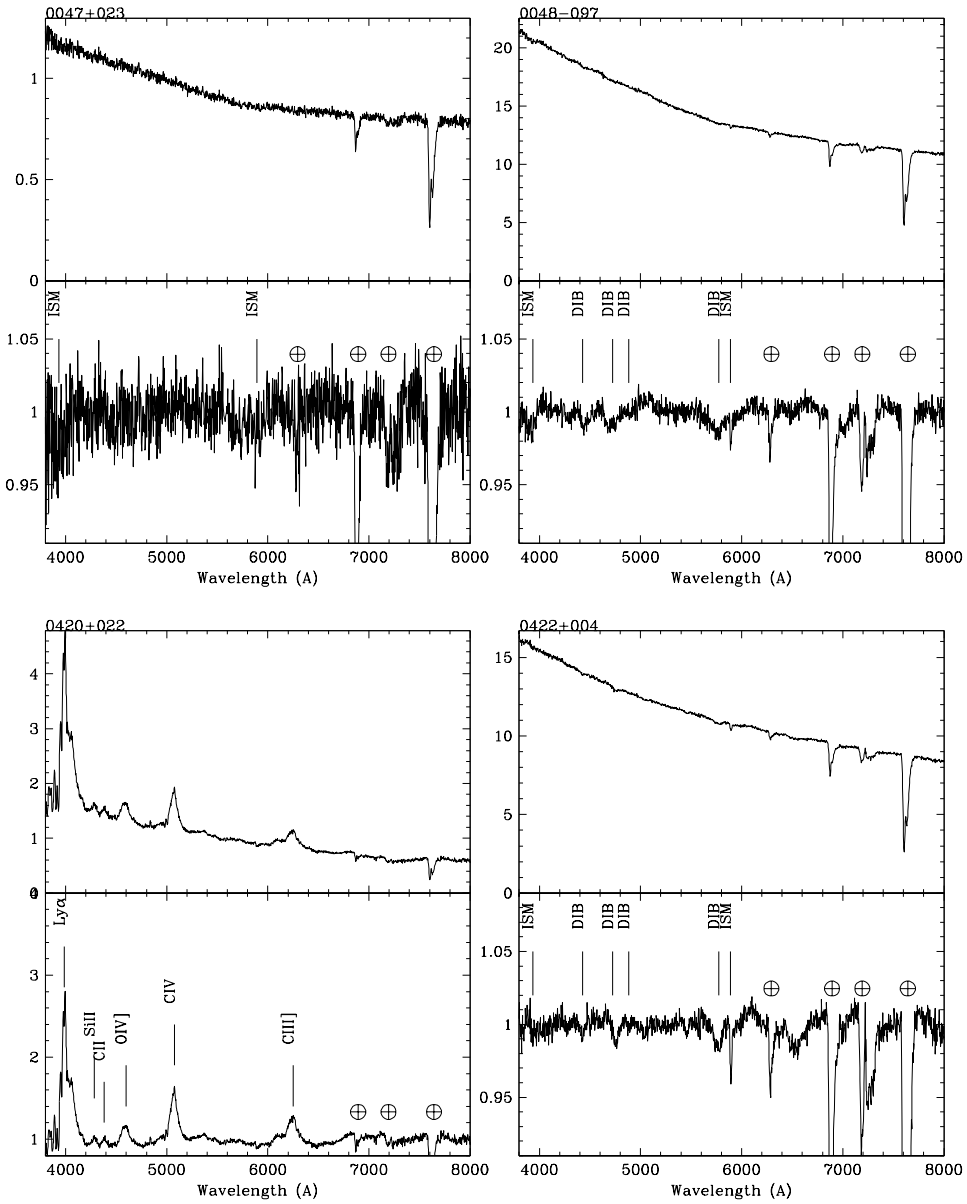

Fig. 2.— Spectra of the observed objects. Top panels: flux calibrated dereddened spectra. Bottom panels: normalized spectra. Telluric bands are indicated by ⊕, spectral lines are marked by the line identification,intervening MgII absorption systems are reported as "int. MgII", unidentified intervening systems are indicated with *, absorption features from atomic species in the interstellar medium of our galaxy are labeled by ISM, diffuse interstellar bands by DIB.

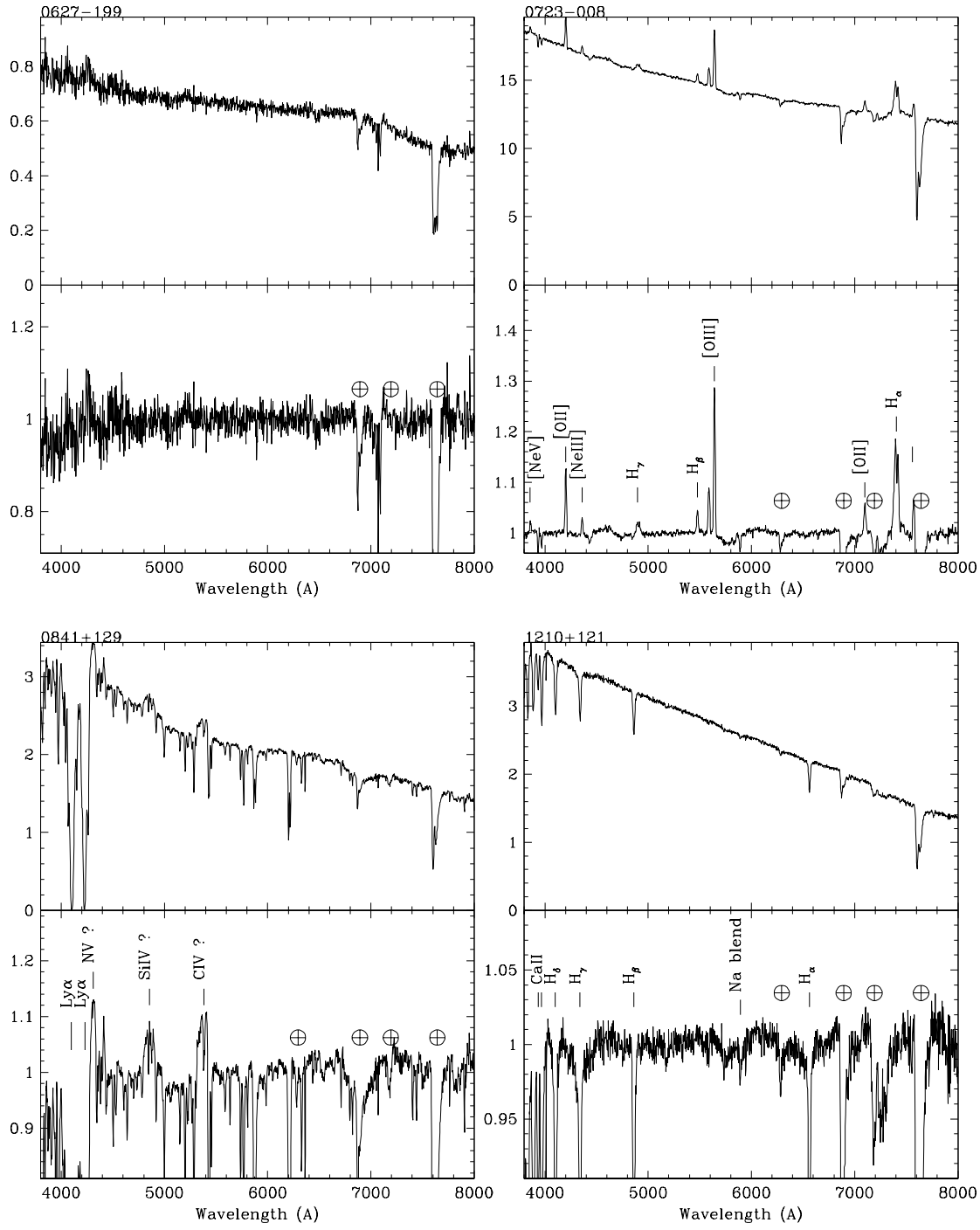

Fig. 2.— continued

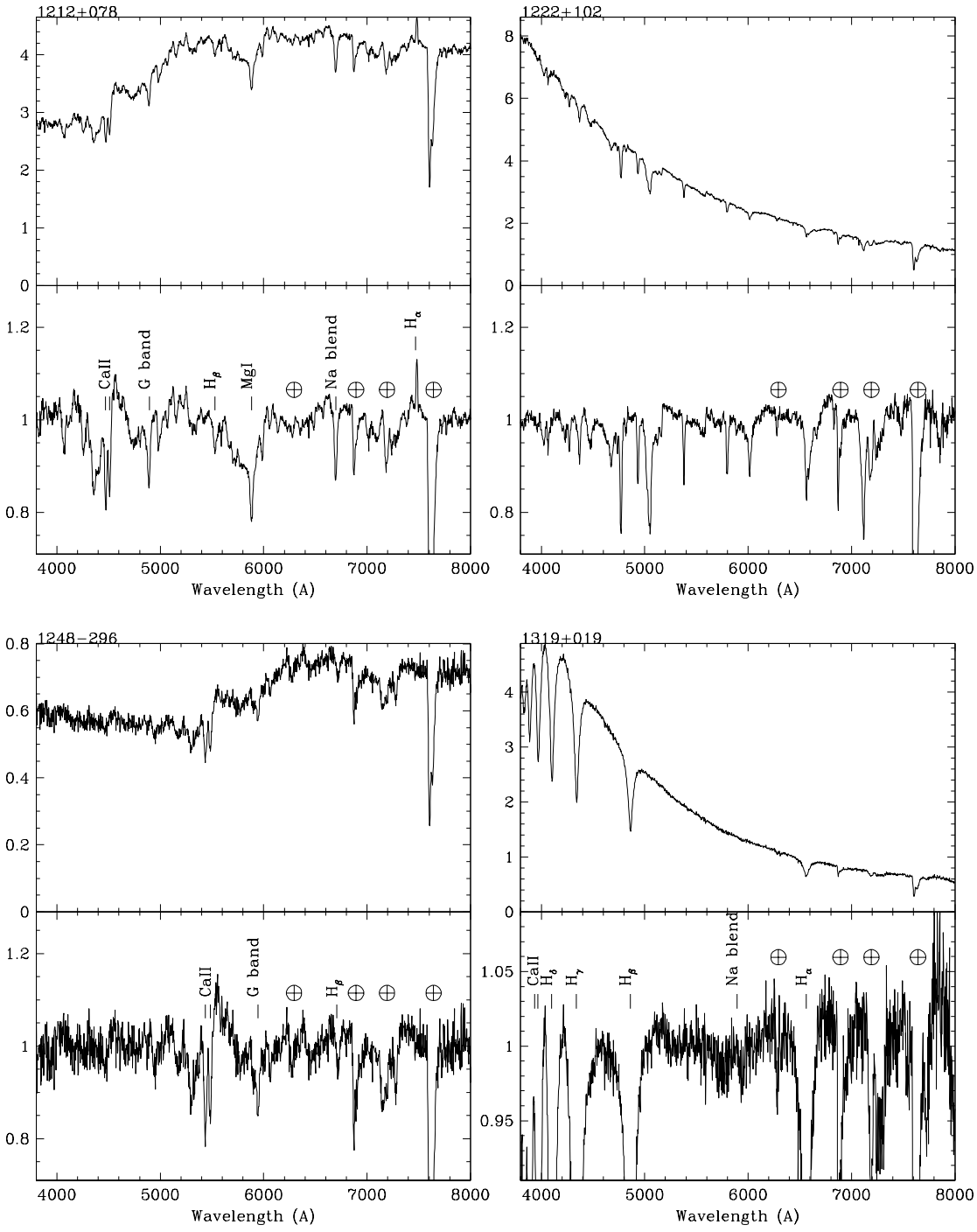

Fig. 2.— continued

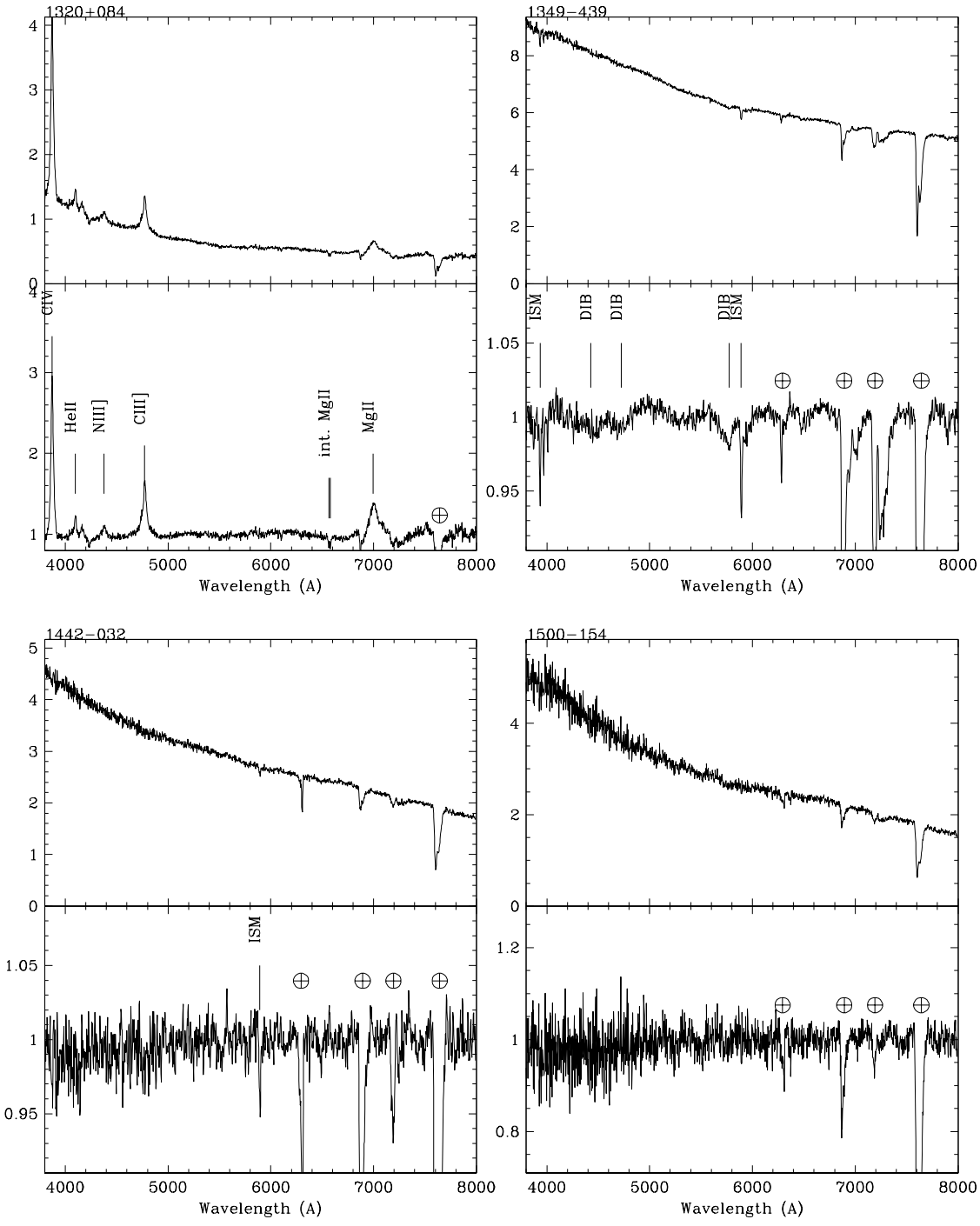

Fig. 2.— continued

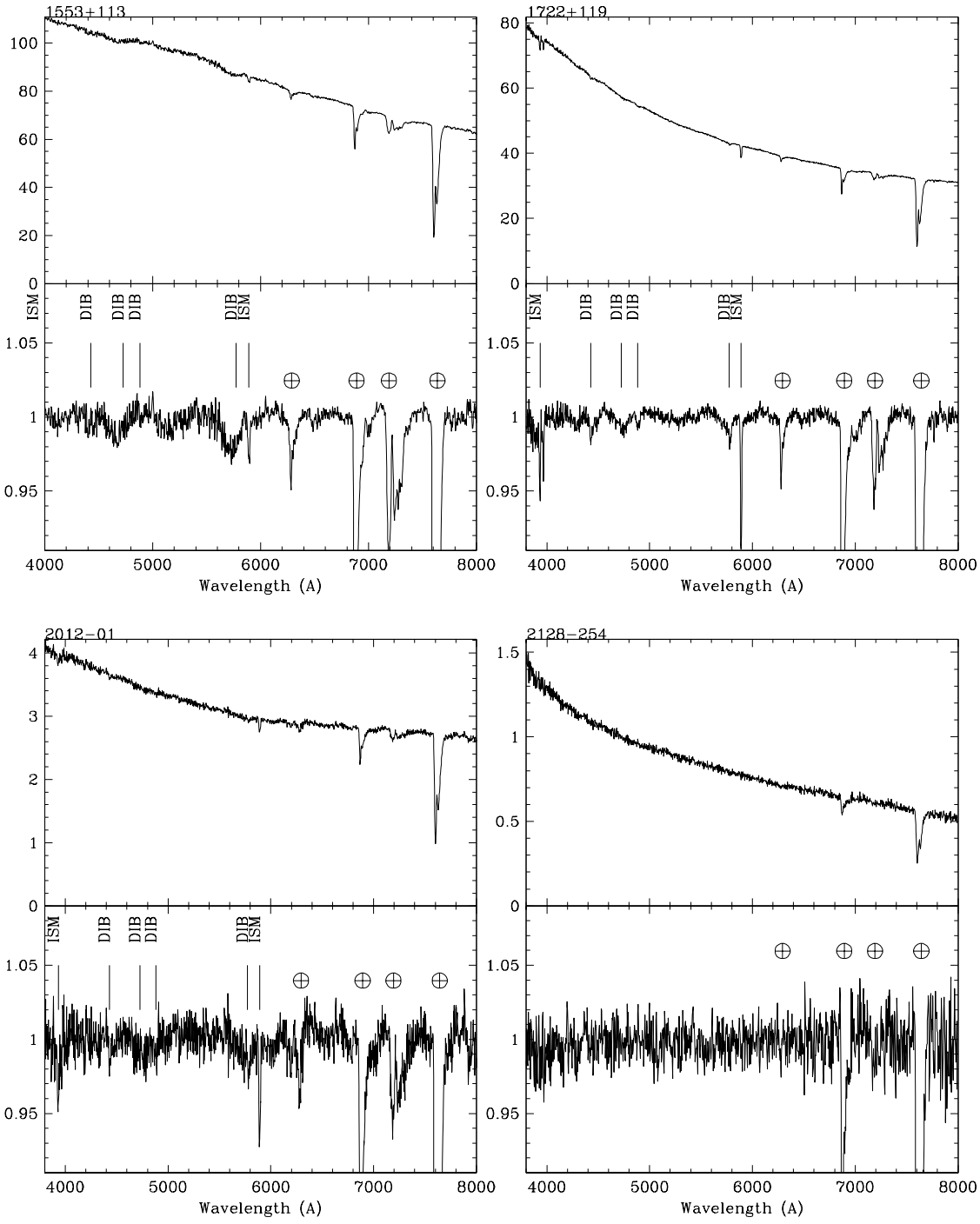

Fig. 2.— continued

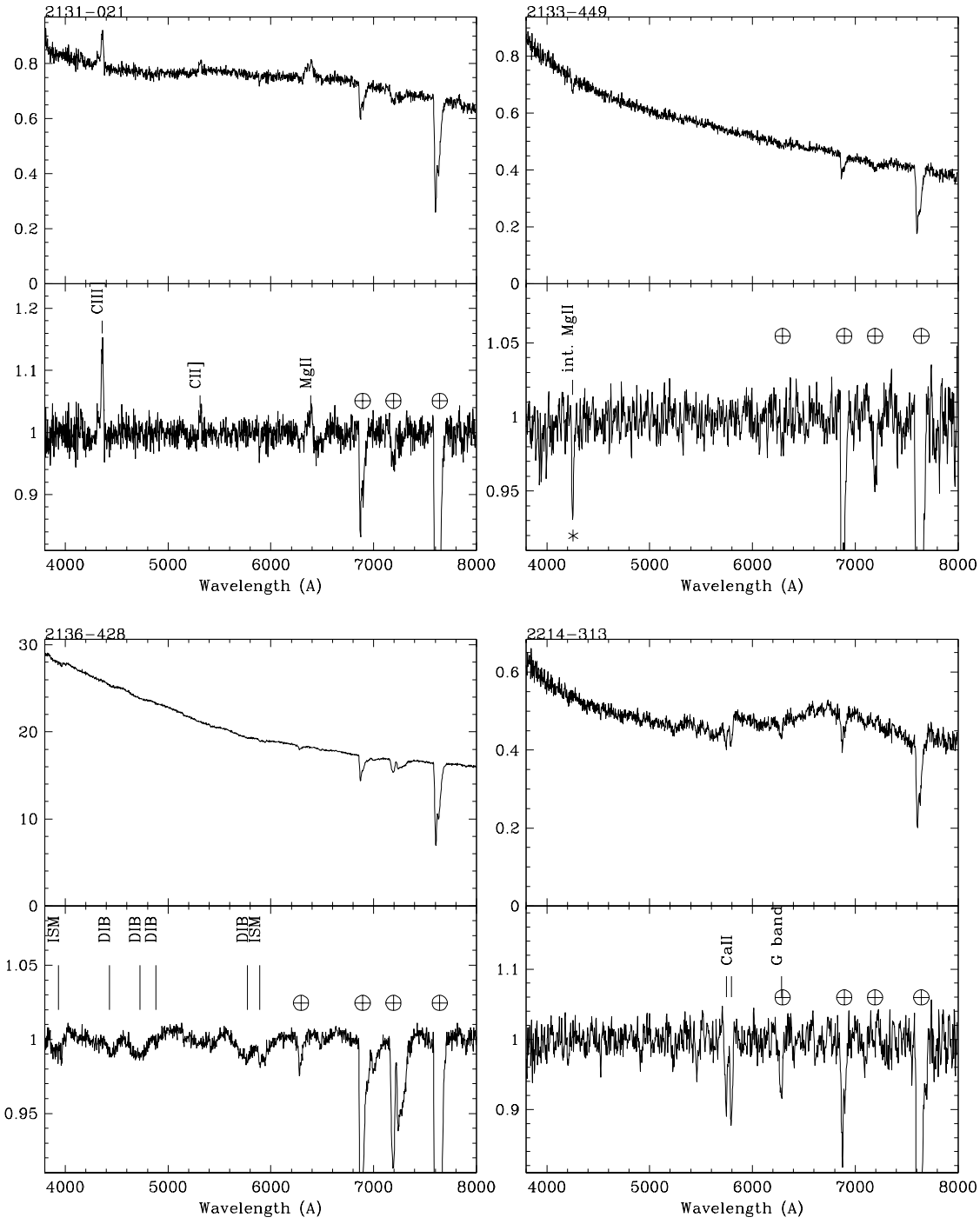

Fig. 2.— continued

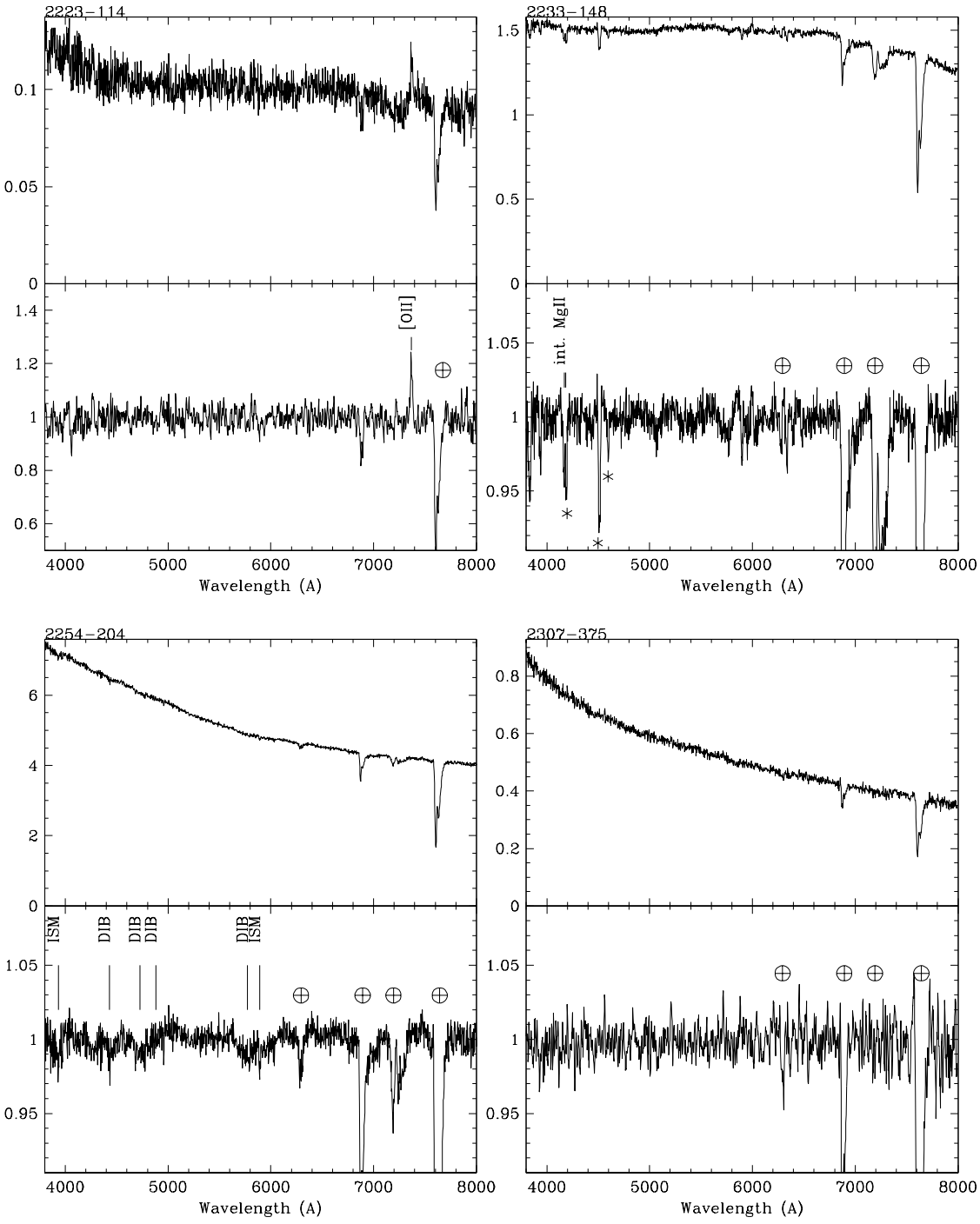

Fig. 2.— continued

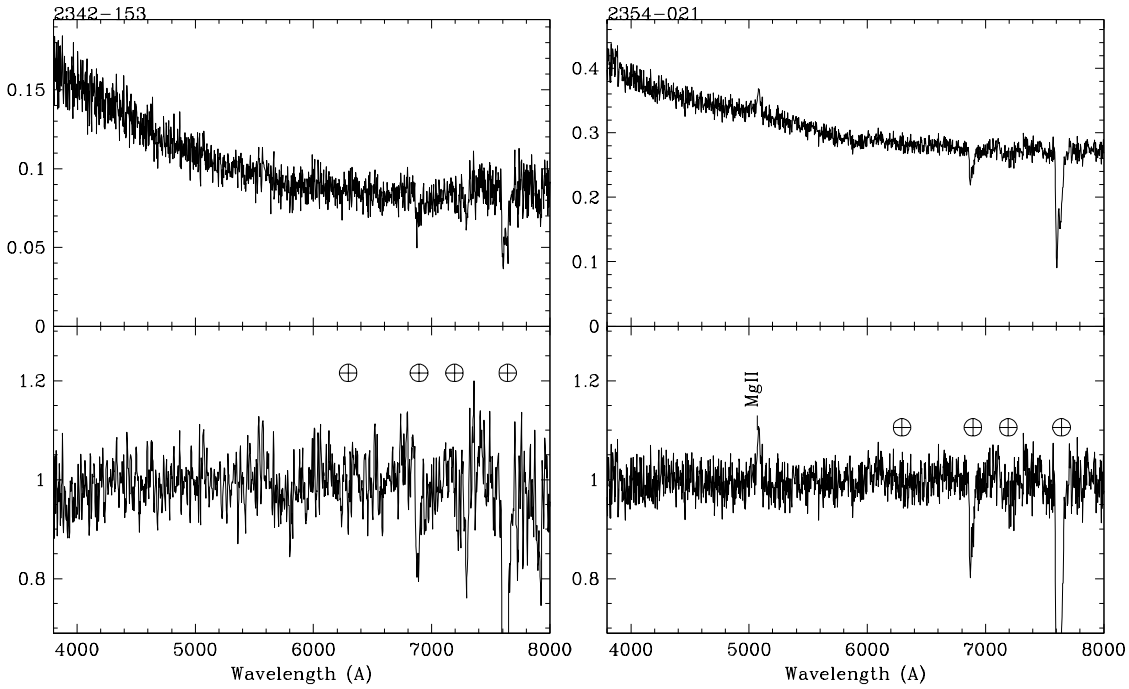

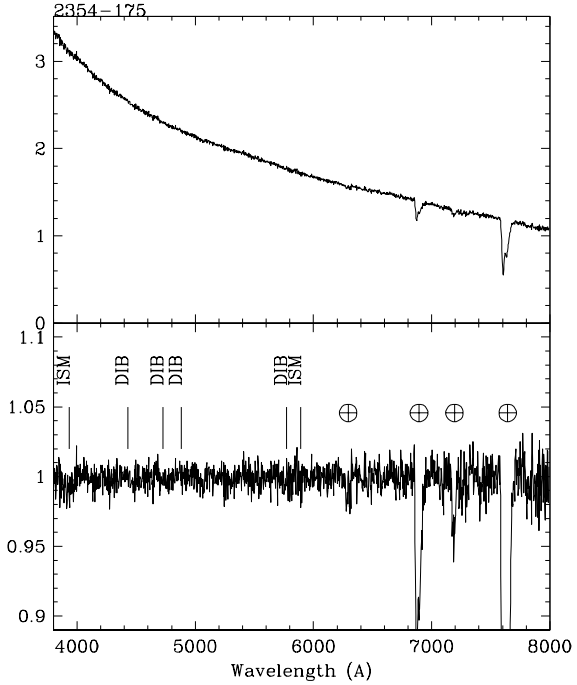

Fig. 2.— continued

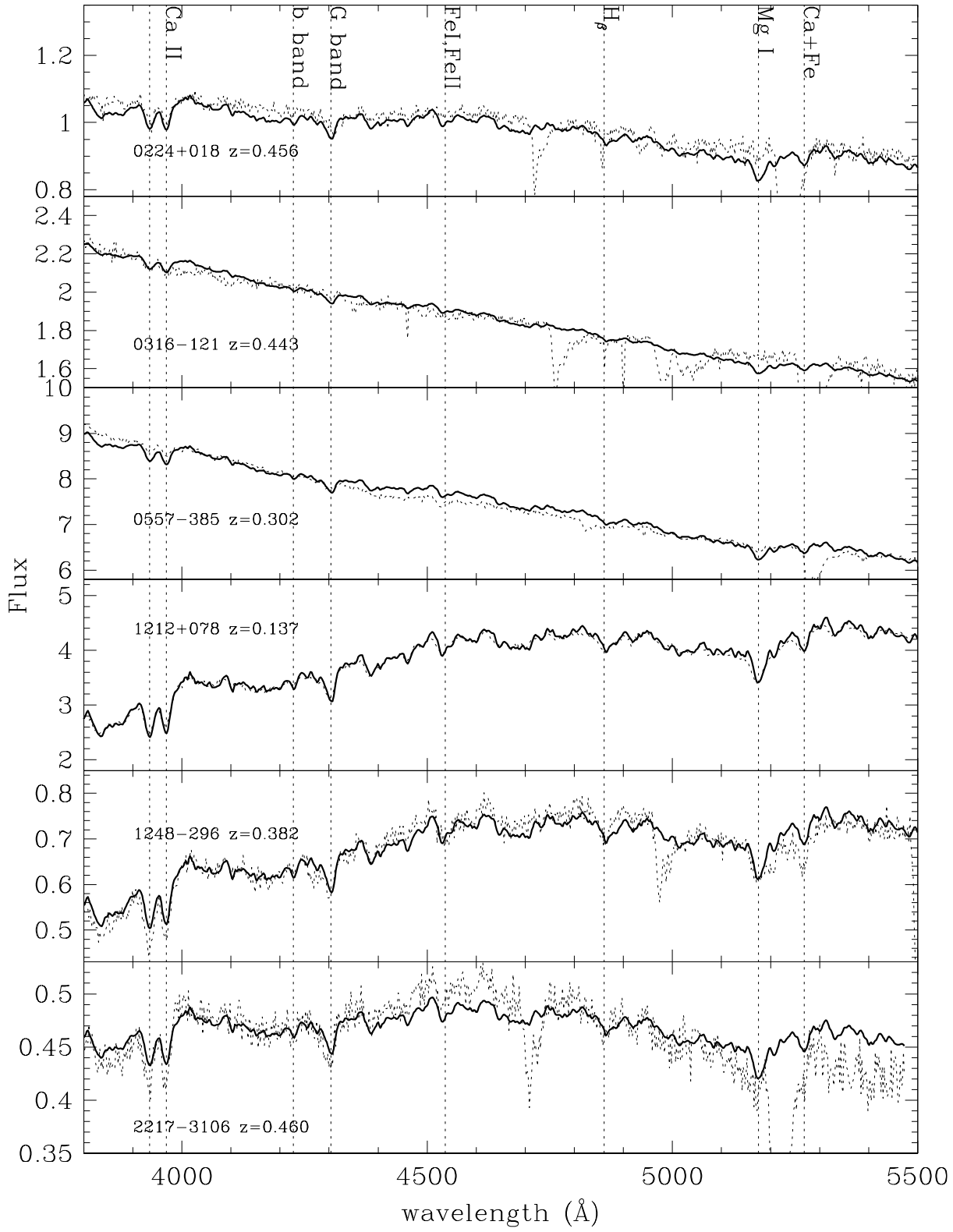

Fig. 3.— Spectral decomposition for objects with detected host galaxy spectral features in the objects rest frame. Solid line shows the fitted spectrum, dotted line the observed one. Objects 0224+018, 0316-121, 0557-385 were discussed in paper I.

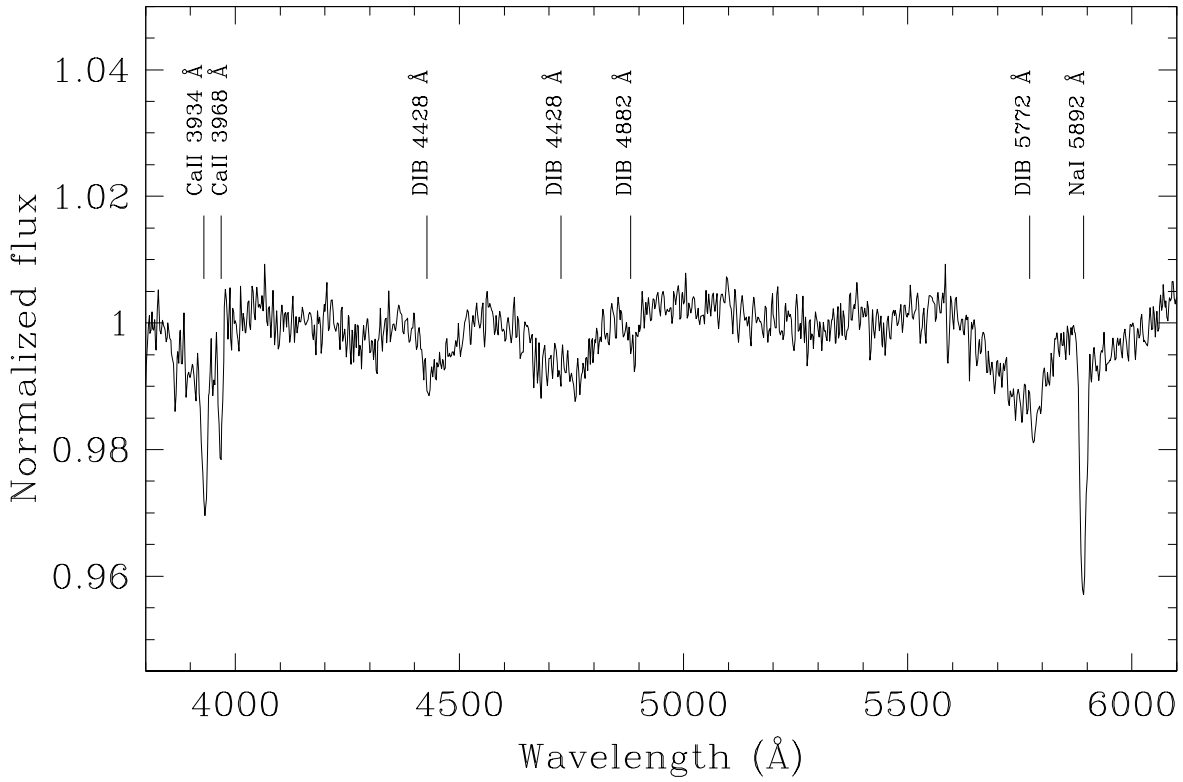

Fig. 4.— Combined spectrum of the ISM features of lineless BL Lacs. CaII $\lambda\lambda$3934,3968 and NaI λ5892 atomic lines and, diffuse interstellar bands (DIB) at $\lambda\lambda$4428,4726,4882,5772 are indicated

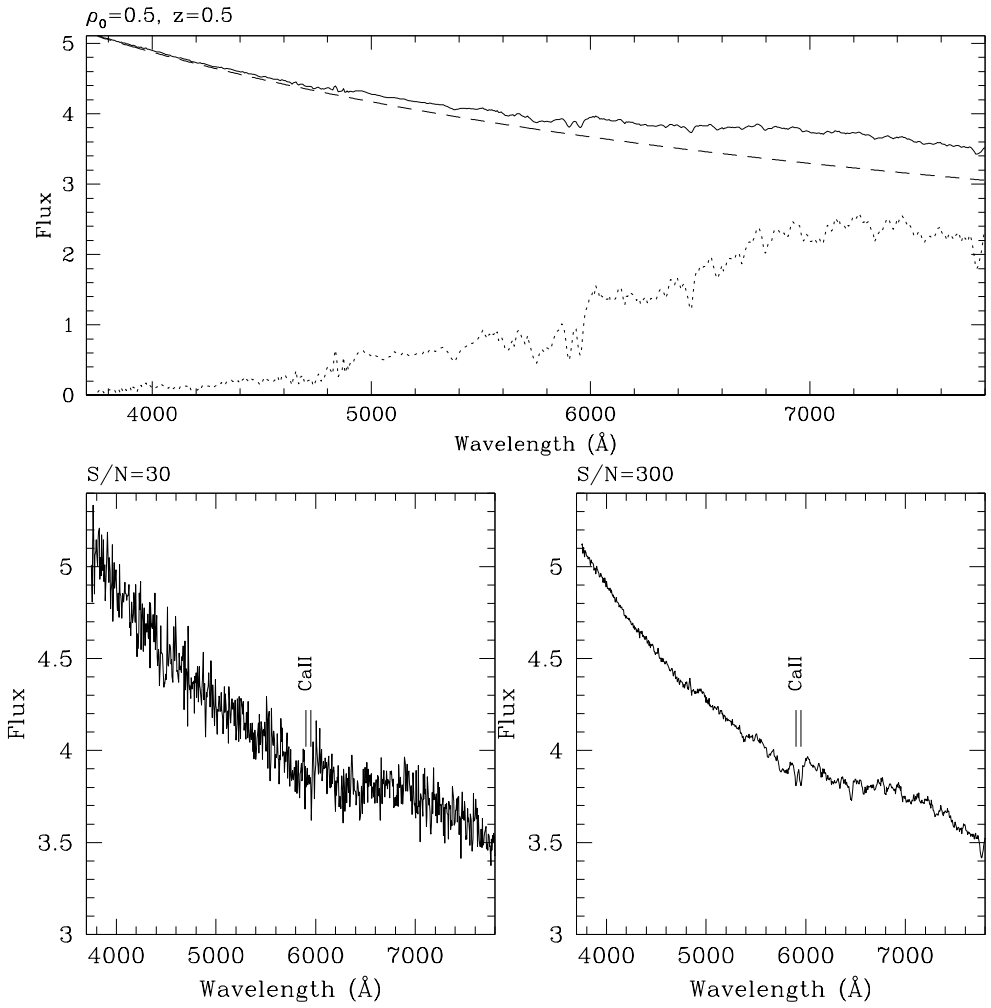

Fig. 5.— *Top panel:* Simulated BL Lac spectrum at z=0.5 (thick line), obtained as the composition of a non-thermal power-law (dashed line) and an elliptical galaxy spectrum (magnified 5 times, dotted line), with nucleus–to–host ratio of 5. *Bottom panels:* the simulated spectrum, if observed with S/N=30 *(left)* or with S/N=300 *(right)*

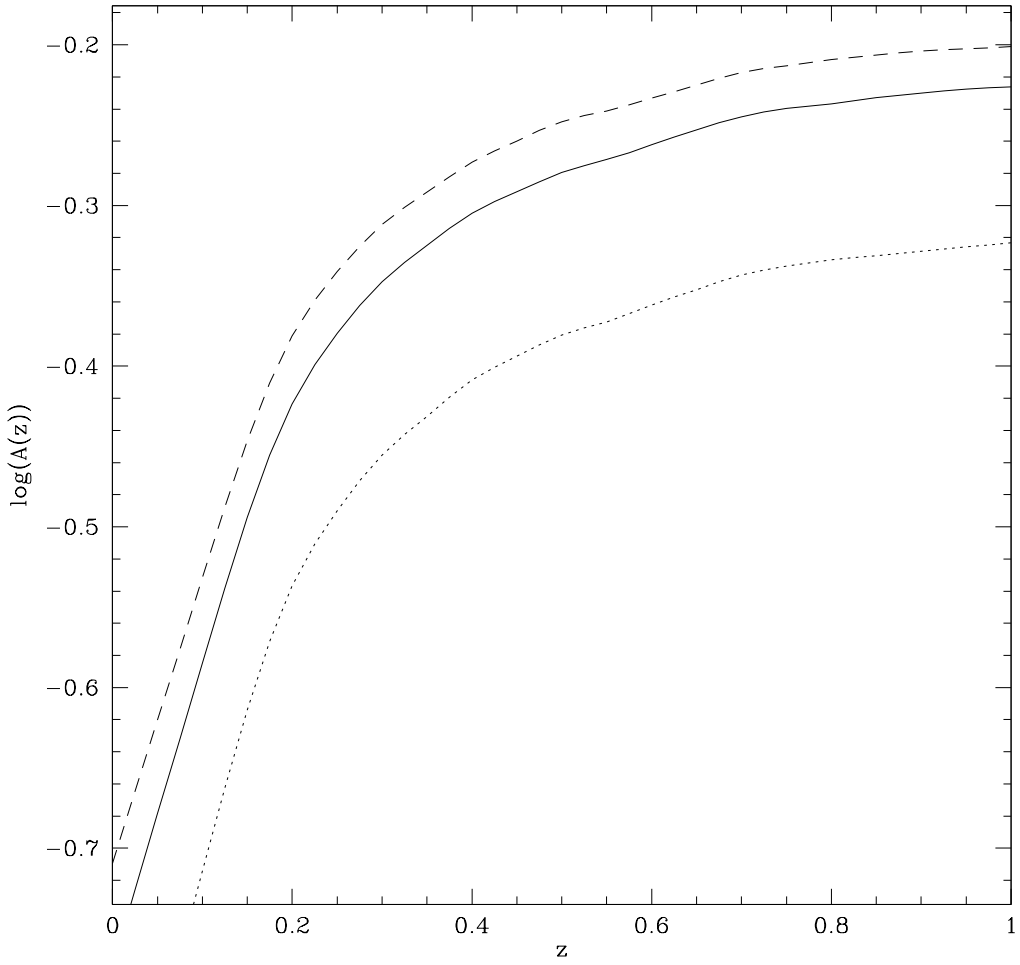

Fig. 6.— Aperture effect correction A(z) as a function of the redshift for aperture sizes 2"×12" (dashed), 2"×6" (solid), 2"×3" (dotted). Seeing is assumed to be ∼1".

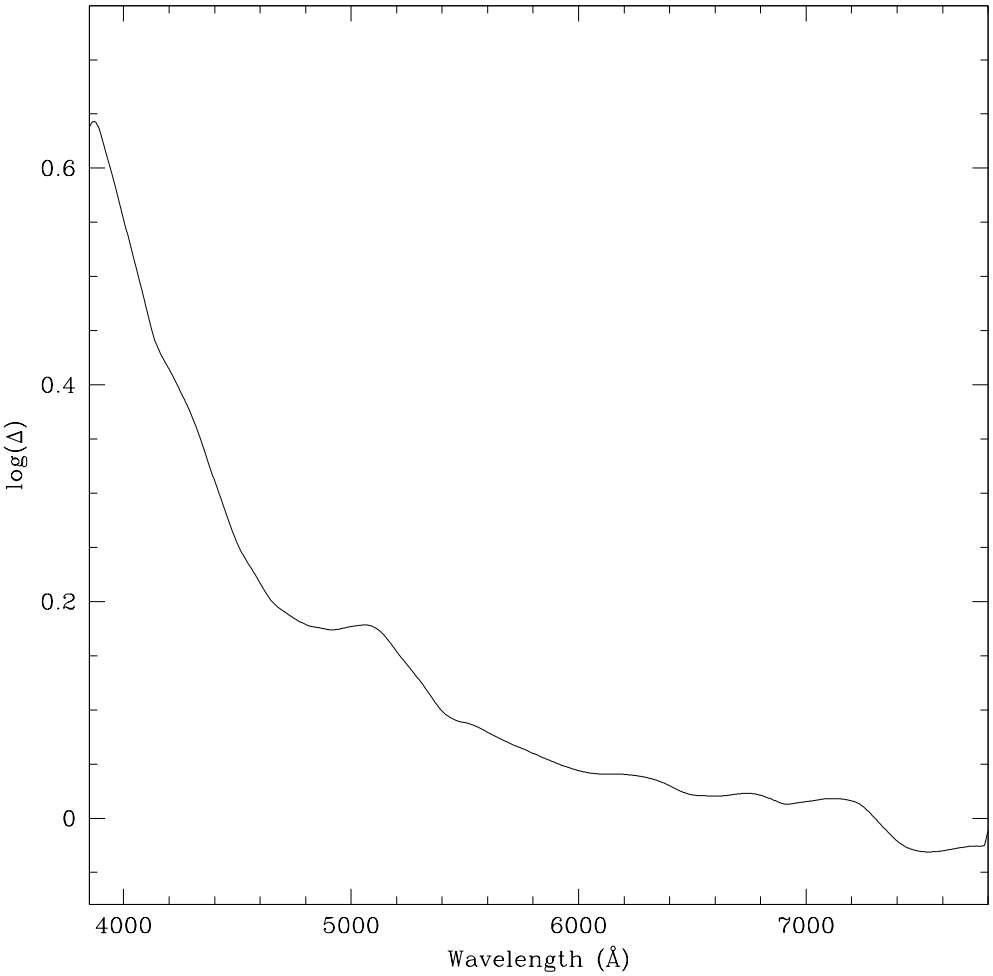

Fig. 7.— Relative nucleus–to–host ratio Δ, referred to λ_0=6750 Å(effective wavelength for R band magnitude), as a function of the wavelength. The assumed spectral index for the nuclear component is α=0.7. For CaII λ3934 absorption feature, Δ equals 4.3.

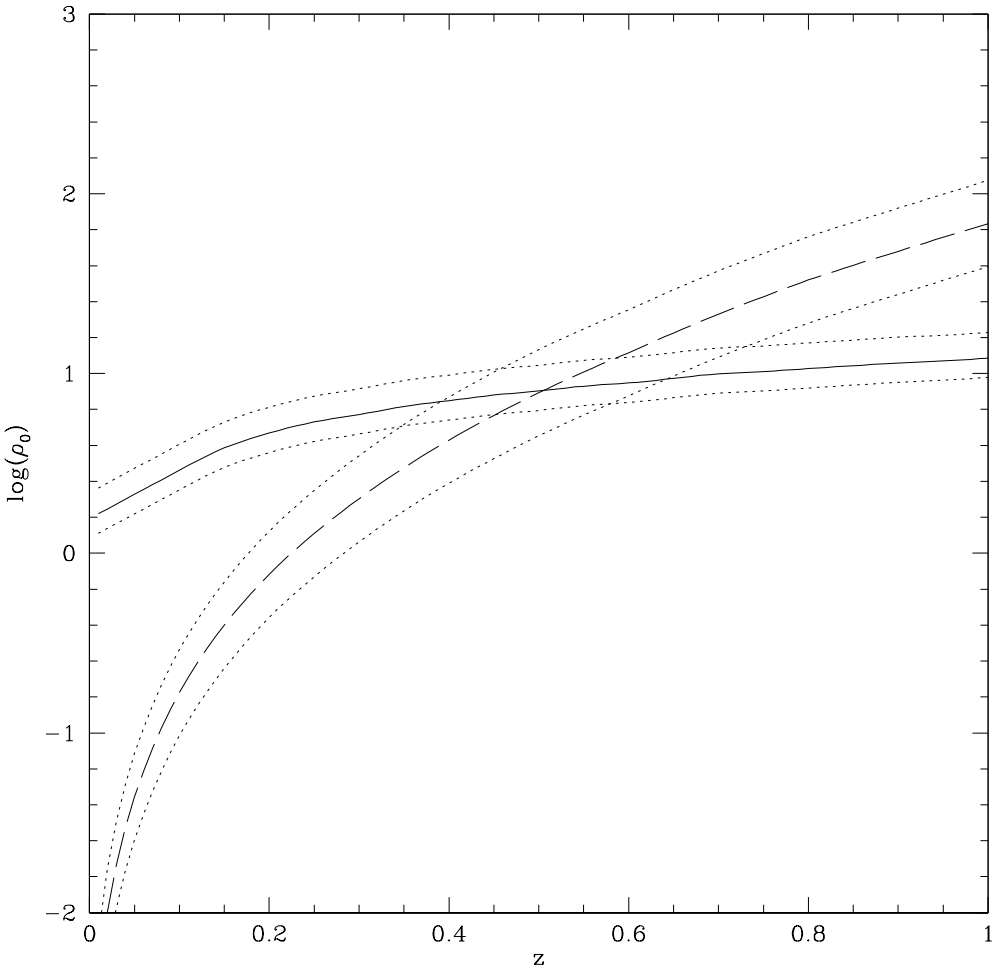

Fig. 8.— Redshift lower limit obtained from apparent magnitude and EW_{min} values for 1RXS J150343.0−154107. The thick solid line represents the N/H vs z limit obtained from the EW_{min} value. Dotted curves correspond to a 0.1 Å uncertainty on EW_{min}. The dashed line gives the N/H vs. z relation for a BL Lac with a host galaxy with M_R=-22.9 and nuclear apparent magnitude R=17.7. Dotted lines correspond to the uncertainty due to the range of variation of host galaxy magnitude (0.5 mag) and observational photometric errors (0.1 mag). The intersection between the two solid lines gives the lower limit on the redshift. The analytic form of the curves is described by Eqs. 3, 4; further details can be found in Sbarufatti (2005)

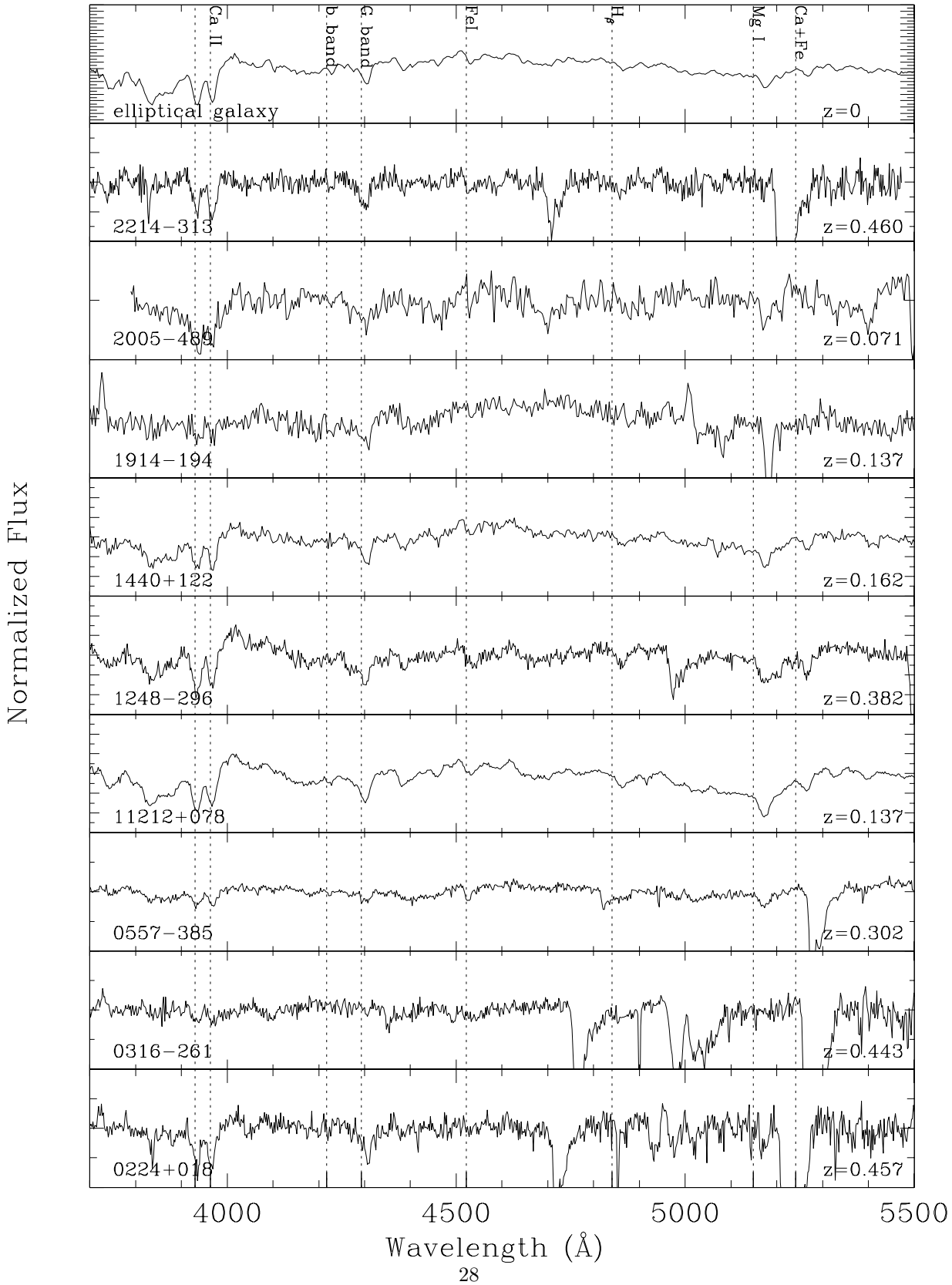

Fig. 9.— Rest Frame normalized spectra of objects used to compare redshift estimates from CaII equivalent widths with spectroscopic values.

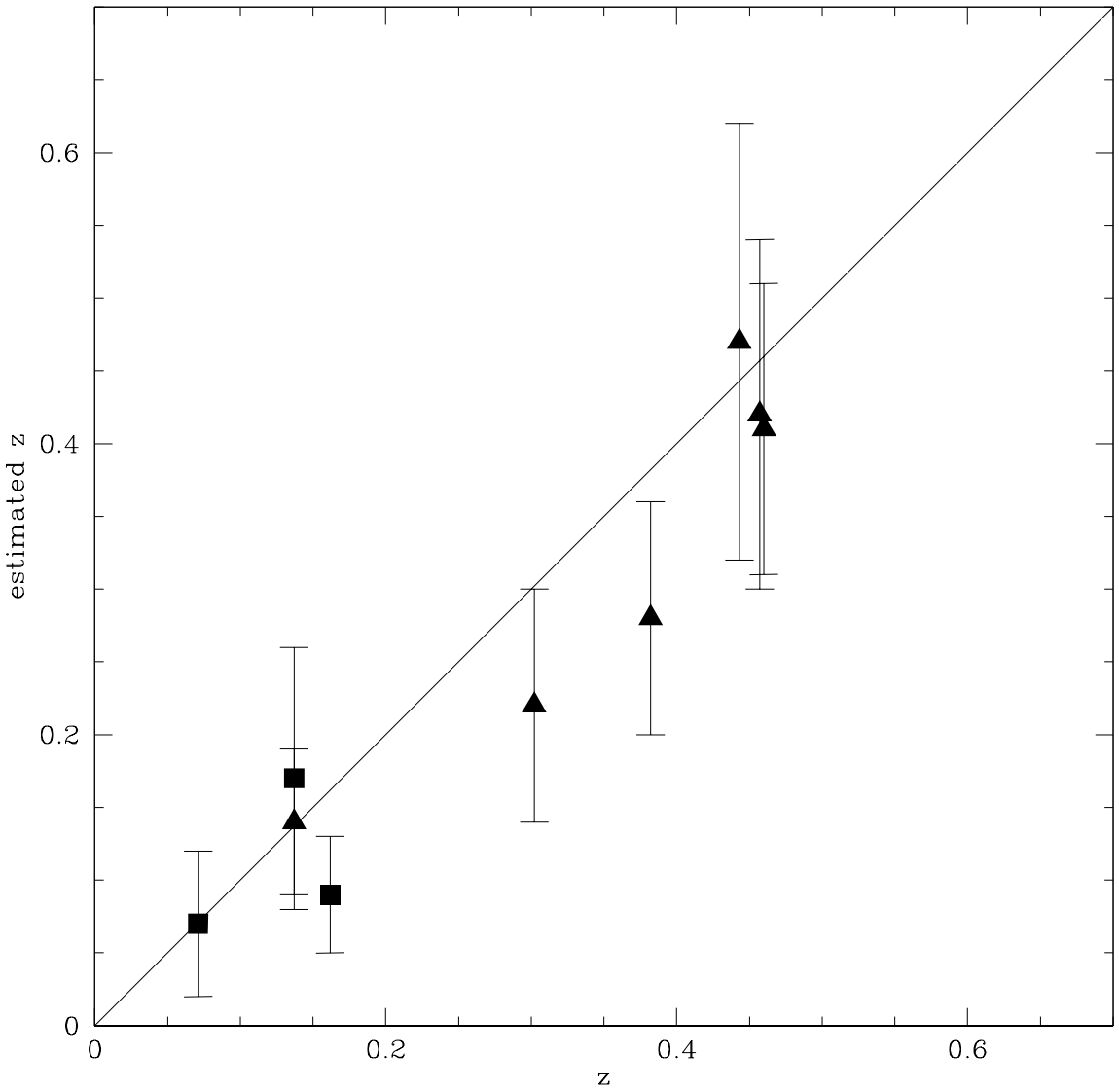

Fig. 10.— Comparison between the spectroscopic redshift z and the value estimated from CaII equivalent widths (see section 4.2.4 and Fig. 8). Triangles refer to objects observed at ESO 3.6m, squares to objects observed at ESO VLT (this work).

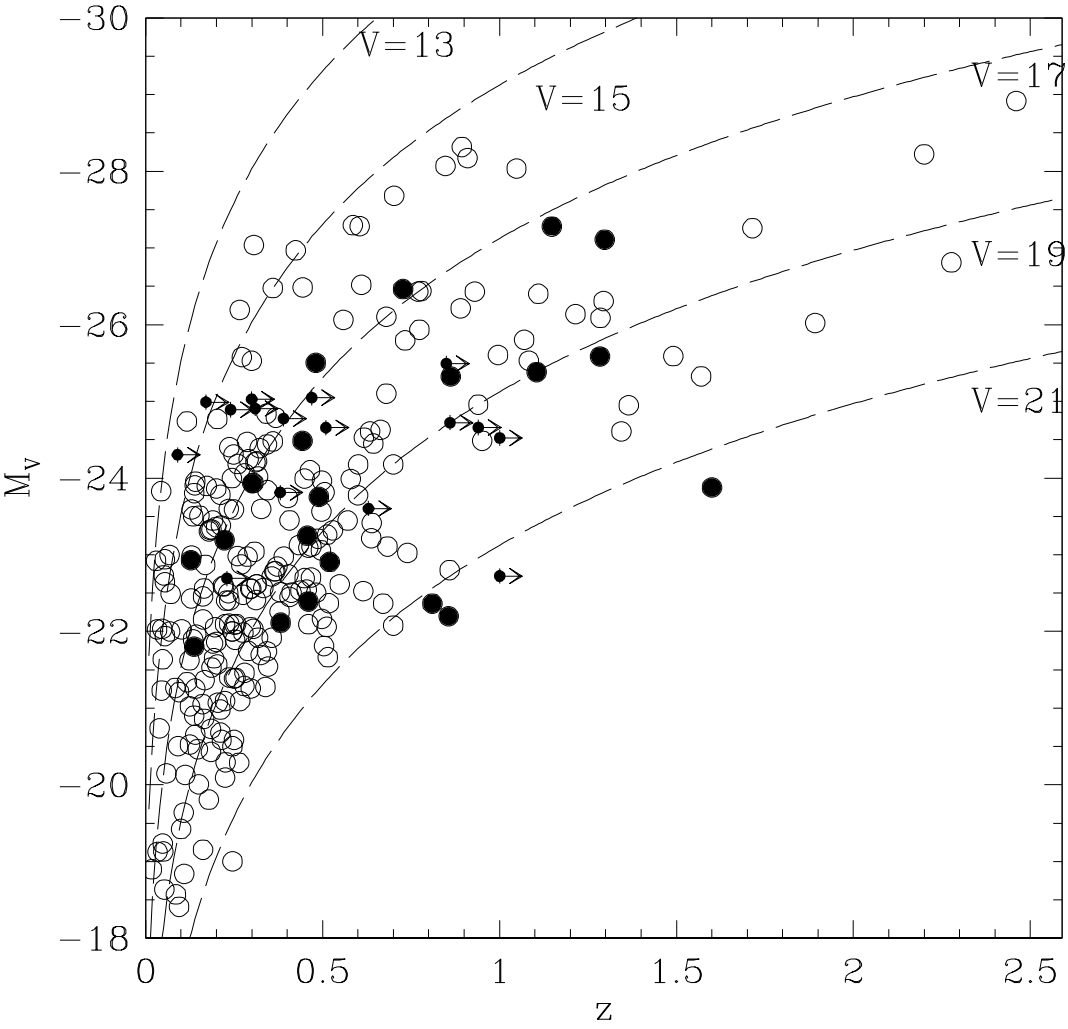

Fig. 11.— M_V vs. redshift distribution of : Padovani & Giommi (1995a) + SS sample with redshift known from literature (open circles), BL Lacs the redshift of which has been determined in paper I and in this work (filled circles), including redshift lower limits (arrows).

Table 1

Journal of observations and results for objects not reported in paper I

Object name (1)	IAU name (2)	RA (J2000) (3)	Dec (J2000) (4)	Date (5)	t_{exp} (6)	S/N (7)	R (8)	α (9)	EW_{min} (10)	z (11)
PKS 0047+023	0047+023	00 49 43.2	+02 37 04.8	05 Aug 03	1800	80	19.0	0.61	0.36	>0.82
PKS 0048−09	0048−097	00 50 41.3	−09 29 05.2	17 Sep 03	1800	250	16.0	0.95	0.22	>0.30
PKS 0420+022	0420+022	04 22 52.2	+02 19 26.9	19 Nov 03	2325	90	18.9	*	0.41	2.278
PKS 0422+00	0422+004	04 24 46.8	+00 36 06.3	27 Nov 03	2325	230	16.2	0.88	0.25	>0.31
PKS 0627−199	0627−199	06 29 23.8	−19 59 19.7	16 Dec 03	2325	50	19.3	0.56	0.92	>0.63
PKS 0723−00	0723−008	07 25 50.6	−00 54 56.5	25 Dec 03	2325	250	16.0	*	0.23	0.127
H 0841+1256	0841+129	08 44 24.1	+12 45 48.0	30 Dec 03	2325	100	18.0	*	0.38	>2.48
HB89 1210+121	1210+121	12 12 33.9	+11 50 56.9	24 Jan 04	2325	180	17.8	*	0.28	*
1ES 1212+078	1212+078	12 15 10.9	+07 32 03.8	25 Jan 04	2325	100	17.3	1.17	0.39	0.137
1222+102	1222+102	12 25 23.1	+09 59 35.0	26 Jan 04	2325	160	17.7	2.67	0.30	*
1ES 1248−296	1248−296	12 51 34.9	−29 58 42.9	24 Jan 04	2325	50	19.5	0.92	0.57	0.382
UM566	1319+019	13 19 55.1	+01 52 58.3	30 Apr 03	1800	100	18.2	*	0.36	*
1ES 1320+084N	1320+084	13 22 54.9	+08 10 10.0	30 Apr 03	2325	50	19.5	*	0.54	1.500
PKS 1349−439	1349−439	13 52 56.5	−44 12 40.4	30 Apr 03	1800	240	16.9	0.82	0.32	>0.39
1RXS J144505.9−032613	1442−032	14 45 05.8	−03 26 12.8	28 Aug 04	2325	100	17.7	1.21	0.35	>0.51
1RXS J150343.0−154107	1500−154	15 03 42.9	−15 41 07.0	28 Aug 04	2325	40	17.8	1.52	0.78	>0.38
HB89 1553+113	1553+113	15 55 43.0	+11 11 24.4	01 Aug 03	1800	250	14.0	0.84	0.25	>0.09
H 1722+119	1722+119	17 25 04.4	+11 52 15.2	06 Apr 03	1800	350	14.7	1.30	0.18	>0.17
PKS 2012−017	2012−017	20 15 15.2	−01 37 33.0	31 Jul 03	1800	130	19.3	0.49	0.34	>0.94
1RXS J213151.7−251602	2128−254	21 31 51.6	−25 16 00.8	10 Jul 04	2325	70	19.0	1.28	0.32	>0.86
PKS 2131−021	2131−021	21 34 10.3	−01 53 17.0	18 Jul 04	2325	80	19.2	0.29	0.43	1.284
MH 2133−449	2133−449	21 36 18.4	−44 43 49.0	12 Jul 04	2325	60	19.5	1.02	0.37	>0.98
MH 2136−428	2136−428	21 39 24.1	−42 35 21.3	03 Jul 03	1800	490	15.6	0.84	0.24	>0.24
RX J22174−3106	2214−313	22 17 28.4	−31 06 19.0	10 Jul 04	2325	50	19.7	0.90	0.68	0.460
PKS 2223−114	2223−114	22 25 43.6	−11 13 40.0	02 Sep 04	2325	20	21.5	0.31	1.04	0.997
PKS 2233−148	2233−148	22 36 34.0	−14 33 21.0	02 Sep 04	2325	170	18.5	0.15	0.30	>0.65
PKS 2254−204	2254−204	22 56 41.2	−20 11 40.3	31 Jul 03	1800	220	17.1	0.86	0.25	>0.47
1RXS J231027.0−371926	2307−375	23 10 26.9	−37 19 26.0	10 Jul 04	2325	80	19.6	1.15	0.34	>1.03
MS 2342.7−1531	2342−153	23 45 22.4	−15 15 06.7	26 Jul 03	2325	20	21.4	1.02	1.72	>1.03
1RXS J235730.1−171801	2354−175	23 57 29.7	−17 18 05.3	12 Jul 04	2325	150	18.2	1.44	0.17	>0.85

Note.—Description of columns: (1) Object name; (2) IAU name; (3) Right Ascension (J2000); (4) Declination (J2000); (5) Date of observations; (6) Exposure time (seconds); (7) Signal to Noise; (8) Seeing during observations; (9) Spectral index of the continuum, α, defined by $F_\lambda \propto \lambda^{-\alpha}$; (10) Minimum detectable EW; (11) Redshifts measured from spectral features and redshift lower limits from the procedure described in section 4.2.3.

Table 2

Parameters of BL Lac spectral decomposition

Object (1)	z (2)	α (3)	m_R^{host} (4)	M_R^{host} (5)	ρ_0 (6)	M_{phot}^{host} (7)	Note (8)
0224+018	0.456	1.50	19.9	−23.2	2.2	−23.1	(1)
0316−121	0.443	1.44	20.2	−22.8	6.4		(1)
0557−385	0.302	1.61	18.3	−23.4	5.5		(1)
1212+078	0.137	1.17	17.4	−22.0	0.4	−23.0	
1248−296	0.382	0.92	19.7	−22.7	0.8	−23.7	
2214−313	0.460	0.90	20.8	−22.3	2.1		

Note.—Description of columns: (1) Object name (2) Redshift (3) Fitted spectral index of the continuum, α, defined by $F_\lambda \propto \lambda^{-\alpha}$; (4) fitted R magnitude of the host galaxy; (5) Absolute R magnitude of the host galaxy, corrected for extinction and evolution, but not for aperture effects; (6) Rest frame R band nucleus-to-host flux ratio; (7) Absolute R magnitude of the host galaxy from photometry; (8) Note: (1) Spectrum published in Sbarufatti et al. (2005a).

TABLE 3

MEASUREMENTS OF SPECTRAL LINES

Object name (1)	Object class (2)	z_{avg} (3)	Line ID (4)	λ (5)	z (6)	Type (7)	FWHM (8)	EW (9)
0420+022	QSO	2.278						
			Ly_{alpha}	4020	2.278	e	9400	-73.0
			SiII	4285	2.279	e	3900	-4.0
			CII	4381	2.281	e	5500	-3.0
			SiIV	4587	2.283	e	6300	-24.0
			CIV	5077	2.278	e	4900	-50.0
			CIII]	6250	2.274	e	4500	-45.0
0723−008	QSO/BLL	0.127						
			[NeV]	3858	0.126	e	1100	-0.4
			[OII]	4200	0.127	e	1200	-2.1
			[NeIII]	4359	0.127	e	1300	-0.7
			CaII	4433	0.127	g		0.6
			b band	4477	0.127	g		0.1
			G band	4847	0.127	g		0.1
			H_{γ}	4897	0.128	e	3700	-1.0
			H_{β}	5477	0.127	e	1100	-1.0
			[OIII]	5587	0.127	e	900	-1.9
			[OIII]	5642	0.127	e	900	-5.5
			Mg I	5830	0.127	g		0.4
			NaI	6645	0.127	g		0.1
			[OII]	7098	0.127	e	1000	-1.2
			H_{α}	7402	0.128	e	1900	-8.7
			SII	7561	0.126	e	600	-1.1
1212+078	BLL	0.137						
			CaII	4473	0.137	g		5.7
			CaII	4510	0.137	g		4.8
			G band	4890	0.136	g		5.3
			H_{β}	5529	0.137	g		3.5
			Mg I	5883	0.137	g		16.2
			Na I	6696	0.137	g		3.9
			H_{α}	7481	0.139	e	700	-2.0
1248−296	BLL	0.382						
			CaII	5436	0.382	g	2100	6.1
			CaII	5482		g	1700	4.2
			G band	5942		g	2700	5.6
			H_{β}	6719	0.382	g	1600	1.5

TABLE 3—*Continued*

Object name (1)	Object class (2)	z_{avg} (3)	Line ID (4)	λ (5)	z (6)	Type (7)	FWHM (8)	EW (9)
1320+084	QSO	1.500						
			CIV	3873	1.500	e	2200	1.9
			HeII	4095	1.500	e	1900	-9.0
			?	4234		a		-80.2
			NIII]	4376	1.500	e	2300	-5.8
			CIII]	4770	1.500	e	2200	-40.9
			?	6071		a		0.6
			?	6130		a		1.4
			MgII	6563	1.347	a		1.8
			MgII	6578	1.347	a		1.6
			MgII	7001	1.502	e	6700	-60.0
2131−021	BLL	1.283						
			CIII]	4357	1.283	e	2000	-4.4
			CII]	5312	1.284	e	700	-1.4
			MgII	6383	1.281	e	3000	-3.8
2133−449	BLL	>0.52						
			MgII	4250	0.519	a	2500	1.5
2214−313	BLL	0.460						
			CaII	5746	0.461	g	3000	3.7
			CaII	5792	0.460	g	4300	3.3
			Gband	6280	0.459	g	3200	2.6
2223−114	BLL	0.977						
			[OII]	7367		e	1200	-5.0
2233−148	BLL	>0.49						
			MgII	4165	0.490	a		0.7
			MgII	4183	0.493	a		0.9
			?	4514		a		1.7
			?	4598		a		0.5

NOTE.—Description of columns: (1) Object name; (2) Object class; (3) average redshift; (4) line identification; (5) observed wavelength of line center(Å); (6) redshift of the line; (7) type of the line (**e**: emission line; **g**: absorption line from the host galaxy; **a**: absorption line from intervening systems); (8) FWHM of the line (km s^{-1}); (9) EW of the line (Å);

TABLE 4

COMPARISON BETWEEN SPECTROSCOPIC REDSHIFTS AND ESTIMATES OBTAINED FROM EW_{min} VALUES.

Object name (1)	z (2)	$m_R^{nucleus}$ (3)	EW_{CaII} (4)	z_{est} (5)	$\delta_{z_{est}}$ (6)	Tel. (7)
0224+018	0.457	19.0*	1.7	0.42	0.12	VLT
0316−261	0.443	18.1*	0.6	0.47	0.15	VLT
0557−385	0.302	16.9*	0.9	0.22	0.08	VLT
1212+078	0.137	18.5*	5.7	0.14	0.05	VLT
1248−296	0.382	19.8*	6.1	0.28	0.08	VLT
1440+122	0.162	17.2	3.5	0.09	0.04	ESO3.6
1914−194	0.137	15.8	0.5	0.17	0.09	ESO3.6
2005−489	0.071	14.1	0.4	0.07	0.05	ESO3.6
2214−313	0.460	19.9*	3.7	0.41	0.10	VLT

NOTE.—(1) Object name; (2) Spectroscopic z; (3) Nucleus apparent R magnitude (*: obtained from spectral decomposition); (4) EW of CaII λ3934; (5) Estimated z; (6) Error on estimated z; (7) Telescope used for observations.